nature reviews methods primers

https://doi.org/10.1038/s43586-026-00480-9

Primer

Check for updates

Expansion microscopy

Ha V. Vo[1,12], Rong Xu[1,12], Edward S. Boyden[2,3,4,5,6,7,8] ✉ & Yongxin Zhao[1,9,10,11] ✉

Abstract

Expansion microscopy (ExM) is a sample transformation technique that enables the resolving of nanoscale biological features on ordinary microscopes. By physically expanding biological samples permeated by a hydrogel matrix, ExM effectively overcomes the diffraction limit of light microscopy, enabling nanoscale effective resolution on conventional imaging systems (such as confocal microscopes) without specialized super-resolution optics. Since its inception, ExM has evolved beyond fluorescence microscopy, enhancing the resolution of techniques such as mass spectrometry imaging, Raman imaging and in situ sequencing, by physically decrowding biomolecules. This Primer aims to provide a comprehensive guide to ExM, focusing on both its most common and latest variants. We outline a modular approach for understanding the scope of ExM protocols, as well as for understanding how to optimize or tune ExM for specific biological questions, covering essential laboratory equipment, sample preparation techniques, imaging techniques and computational approaches. Additionally, we discuss strategies for handling and analysing the vast data generated by ExM, highlight key applications across various biological fields, including cellular and structural biology, neuroscience, pathology and microbiology, and address current limitations. Finally, we explore emerging innovations in expansion chemistry, multimodal imaging and automation that will further broaden the impact of ExM across biological and clinical research.

Sections

[1]Department of Biological Sciences, Carnegie Mellon University, Pittsburgh, PA, USA. [2]Department of Brain and Cognitive Sciences, Massachusetts Institute of Technology, Cambridge, MA, USA. [3]Department of Biological Engineering, Massachusetts Institute of Technology, Cambridge, MA, USA. [4]McGovern Institute, Massachusetts Institute of Technology, Cambridge, MA, USA. [5]Koch Institute, Massachusetts Institute of Technology, Cambridge, MA, USA. [6]Center for Neurobiological Engineering, Massachusetts Institute of Technology, Cambridge, MA, USA. [7]Howard Hughes Medical Institute, Cambridge, MA, USA. [8]K. Lisa Yang Center for Bionics and Yang Tan Collective, MIT, Cambridge, MA, USA. [9]Carnegie Mellon Neuroscience Institute, Pittsburgh, PA, USA. [10]Department of Biomedical Engineering, Carnegie Mellon University, Pittsburgh, PA, USA. [11]Viron Molecular Medicine Institute, Boston, MA, USA. [12]These authors contributed equally: Ha V. Vo, Rong Xu. ✉e-mail: edboyden@mit.edu; yongxinz@andrew.cmu.edu

Introduction

For decades, electron microscopy was the primary method used for visualizing nanoscale structures, offering resolution beyond the diffraction limit of light. The advent of super-resolution fluorescence microscopy transformed this landscape by enabling optical imaging of subcellular structures with fine-scale detail and additionally molecular contrast. Super-resolution imaging techniques such as single-molecule localization microscopy (SMLM)[1], stimulated emission depletion (STED) microscopy[2,3] and minimal fluorescence photon fluxes microscopy[4–8], among others, extended the capabilities of traditional light microscopy, bringing molecular-level detail into focus. Despite these advances, challenges remained. For example, these techniques achieved nanometre-scale resolution through optical manipulation strategies, such as point-spread function shaping or localization computation, which required advanced and/or expensive instrumentation. Additionally, these techniques were often too slow for imaging large, intact biological specimens in three dimensions.

Expansion microscopy (ExM) offers a fundamentally different approach to visualizing nanoscale structures, by physically enlarging specimens through a chemical process, effectively bypassing the optical limits of diffraction[9]. Unlike super-resolution methods that rely on complex optics, ExM uses a swellable polymer matrix to isotropically expand biological samples, enabling nanoscale resolution with conventional diffraction-limited microscopes. This physical decrowding of biomolecules not only enhances resolution but also improves accessibility of the biomolecules for downstream chemical analyses, such as antibody staining or in situ sequencing. Typical expansion factors range from 4× to 20× , so that a 300-nm diffraction-limited resolution microscope achieves an effective resolution of ~75 nm to ~15 nm, respectively[9–12]. Additionally, ExM is uniquely suited for imaging large, intact specimens, such as tissues or organoids, in three dimensions without compromising molecular integrity or spatial relationships. However, unlike live-cell super-resolution methods, ExM is limited to fixed specimens, as the expansion process disrupts molecular functions and interactions, from their live state.

The ExM workflow involves four core steps (Fig. 1). During anchoring, molecules of interest are equipped covalently with linkers for later attachment to a polymer matrix. The polymerization step involves permeating the sample by a densely intercalating hydrogel network. This hydrogel polymerizes around and between biomolecules with nanometre-scale spacing and binds to the linkers. During softening, tissue structures are treated to disrupt rigidity (for example, via enzymatic digestion or heat-induced chemical denaturation) so that intrinsic mechanical properties will not impede isotropic expansion. The expansion step involves immersing the hydrogel in water, causing it to swell, physically separating hydrogel-anchored molecules while preserving their spatial relationships.

Since its inception, ExM has seen substantial advancements. These include improvements in the achievable expansion factor and resolution, the types of biomolecules that can be anchored and interrogated, the retention of fluorophores and other labels and compatibility with challenging biological samples, such as vascularized[13] or rigid tissues[13–15]. For this Primer, protein-retention ExM (proExM)[16] and the more recent Magnify[15] are used to illustrate the key steps and underlying principles of ExM. The broader landscape of ExM protocols is also discussed to show how different approaches have been adapted for different samples, expansion factors and imaging goals. ProExM and Magnify are presented to explore specific steps and their rationale, but researchers should select the ExM protocol most suited for their scientific question. ProExM is a simple, robust and widespread protocol for 4.5× expansion, illustrative of a common stand-alone anchoring step. Magnify, a newer variant of ExM, uses a concurrent anchoring strategy, enabling 10× expansion and high retention of diverse biomolecules. Expansion protocols are typically validated, at the time of initial publication, by measuring the distortion and effective resolution. Distortion is measured by comparing pre-expansion and post-expansion images — with pre-expansion imaging commonly done on a classical super-resolution microscope — and is typically quite low; 1–2% over a typical microscopic field of view, sufficient for most studies. Resolution, defined as the distance between two objects that can be cleanly separated in an image, is measured by examining objects of known size and shape. Although the structure of the hydrogel could in principle enable nanoscale resolution of ExM, the practical effective resolution is often limited by the optical resolution of the microscope and the size of the fluorescent label when applied before expansion; if applied after expansion, the size of the fluorescent label has less of a role, because molecular spacing is increased by the expansion factor[9,12,16–21]. By exploring proExM and Magnify as pedagogical test cases, all the steps of ExM can be illustrated, as well as how they can be adapted and validated for new contexts.

ExM is now widely adopted in biological imaging, with use in more than 900 experimental papers and preprints[22], enabling discoveries by revealing nanoscale structures, molecule locations and putative molecular interactions. ExM achieves an effective resolution comparable to (and sometimes exceeding) other super-resolution methods, but with unique advantages in cost, experimental simplicity and accessibility for large-volume imaging. Recent advancements have opened new avenues for multi-omic imaging, bridging nanoscale nuclear morphology with gene expression[23–31]. By enabling nanoscale imaging on conventional optical microscopes, ExM has broadened the scope of biological and clinical research, including neuroscience[32–37], pathology[14,23,38–43] and infectious disease research[44–48], offering new opportunities to study molecular organization with high spatial precision. Ultimately, as biology is driven by interactions at the nanoscale level, the ability to easily visualize molecular organization within its structural context is fundamental to understanding biological mechanisms and developing new therapeutic ideas.

This Primer provides a comprehensive guide to ExM, from fundamental principles to practical applications. We pedagogically focus on widely used methods, including proExM and Magnify, to illustrate core concepts and then highlight other widely used, or recent, innovations and their utility. By emphasizing experimental workflows, data validation and future directions, we aim to equip researchers with the knowledge to apply ExM across diverse biological and perhaps even clinical contexts.

Experimentation

Choosing the appropriate ExM method depends on several factors, including the type of biomolecule to be retained, the desired expansion factor and compatibility with desired staining and imaging techniques. Researchers must consider the trade-offs between pre-expansion and post-expansion labelling, different anchoring strategies and softening approaches to optimize ExM for their specific biological questions. Some protocols prioritize retention of proteins (proExM[16]), nucleic acids (expansion fluorescent in situ hybridization, ExFISH[24]) or lipids (lipid ExM[49]), whereas others such as Magnify[15] and united ExM[28] enable the imaging of multiple biomolecule types in the same sample. Expansion factors typically range from moderate (4–5×) to high (10× or more),

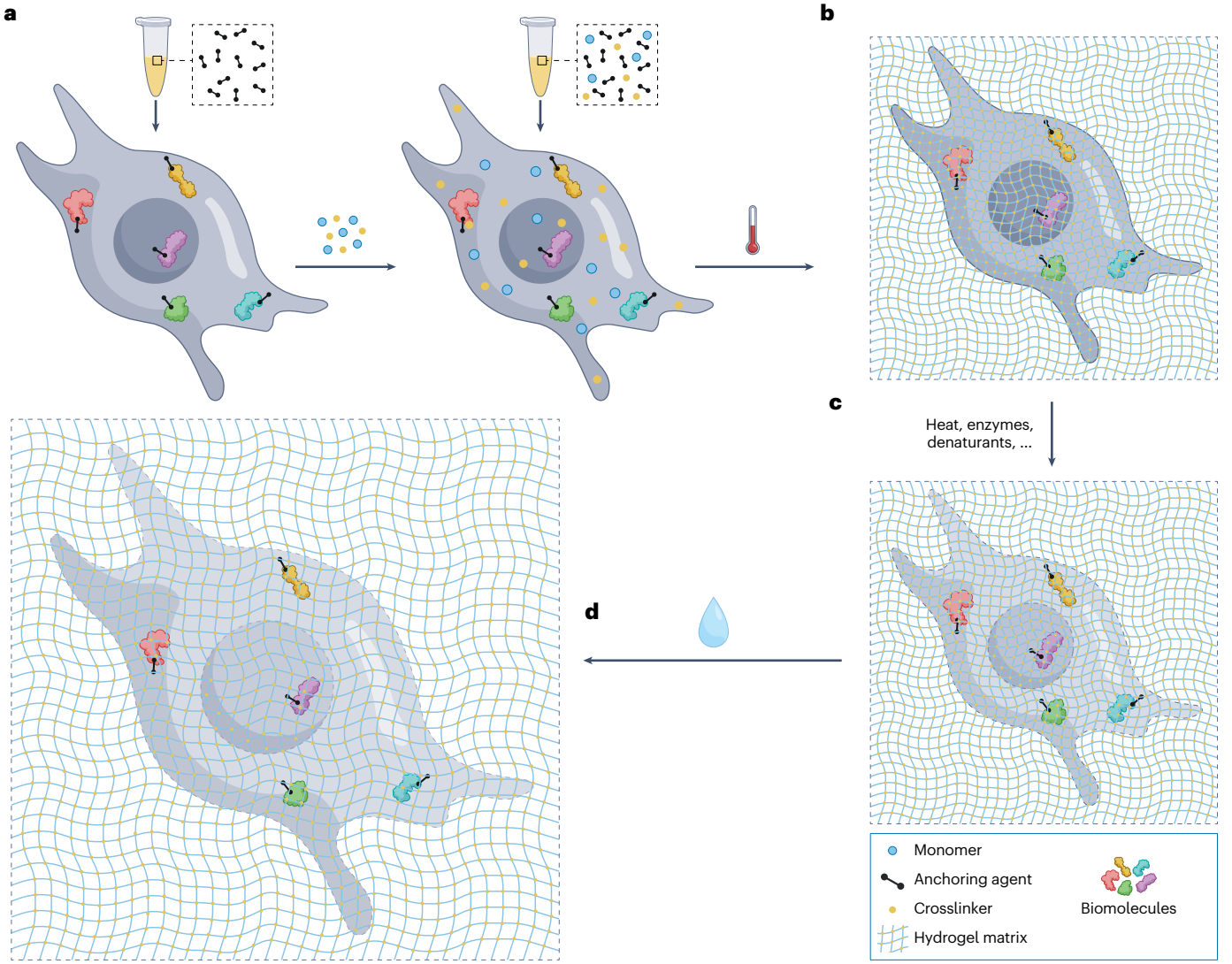

Fig. 1 | Principles of expansion microscopy. The expansion microscopy process consists of four core steps. **a**, Biomolecules of interest are covalently equipped with anchoring agents. This can be done in a separate step before adding hydrogel monomers and crosslinkers (left) or concurrently with the monomer solution (right). **b**, The sample is infused with monomers and crosslinkers that polymerize in situ to form an interpenetrating hydrogel matrix (often triggered by heat), locking the anchored biomolecules to the network. **c**, The sample is mechanically softened through enzymatic or chemical treatment to disrupt its native structure, allowing for uniform expansion. **d**, The hydrogel–sample composite is immersed in water, causing it to swell and physically expand the specimen isotropically by a factor of 4–20×. At one or more points in the process, fluorescent labels can be applied if desired. Not to scale (the mesh size, or spacing between polymer threads, is perhaps 1–2 nm, smaller than many biomolecules).

with iterative strategies extending beyond 16× for applications requiring high resolution. Supplementary Table 1 compares some foundational and/or commonly used ExM protocols (although new protocols are appearing all the time), highlighting widely adopted, robust methods that are straightforward to implement, as well as protocols that introduced key innovations such as targeting diverse biomolecules (such as proteins, nucleic acids and lipids) or higher expansion factors via iterative gelling strategies. Figure 2 outlines typical workflow modules involved in ExM. To illustrate practical implementation and decision-making, the following sections will frequently use proExM (an established protein-retention method) and Magnify (a more recent protocol enabling higher expansion and broader biomolecule retention) as representative examples. Supplementary Table 2 summarizes representative examples of the diverse biological specimens — ranging from cultured cells and microorganisms to complex tissues and whole model organisms — that have been successfully expanded using ExM.

Basic equipment and set-up

ExM relies on a combination of standard laboratory tools and standard reagents to enable sample expansion and high-resolution imaging. Essential equipment includes standard pipettes, incubators, heating blocks, tissue processing tools and gel-casting accessories such as paint

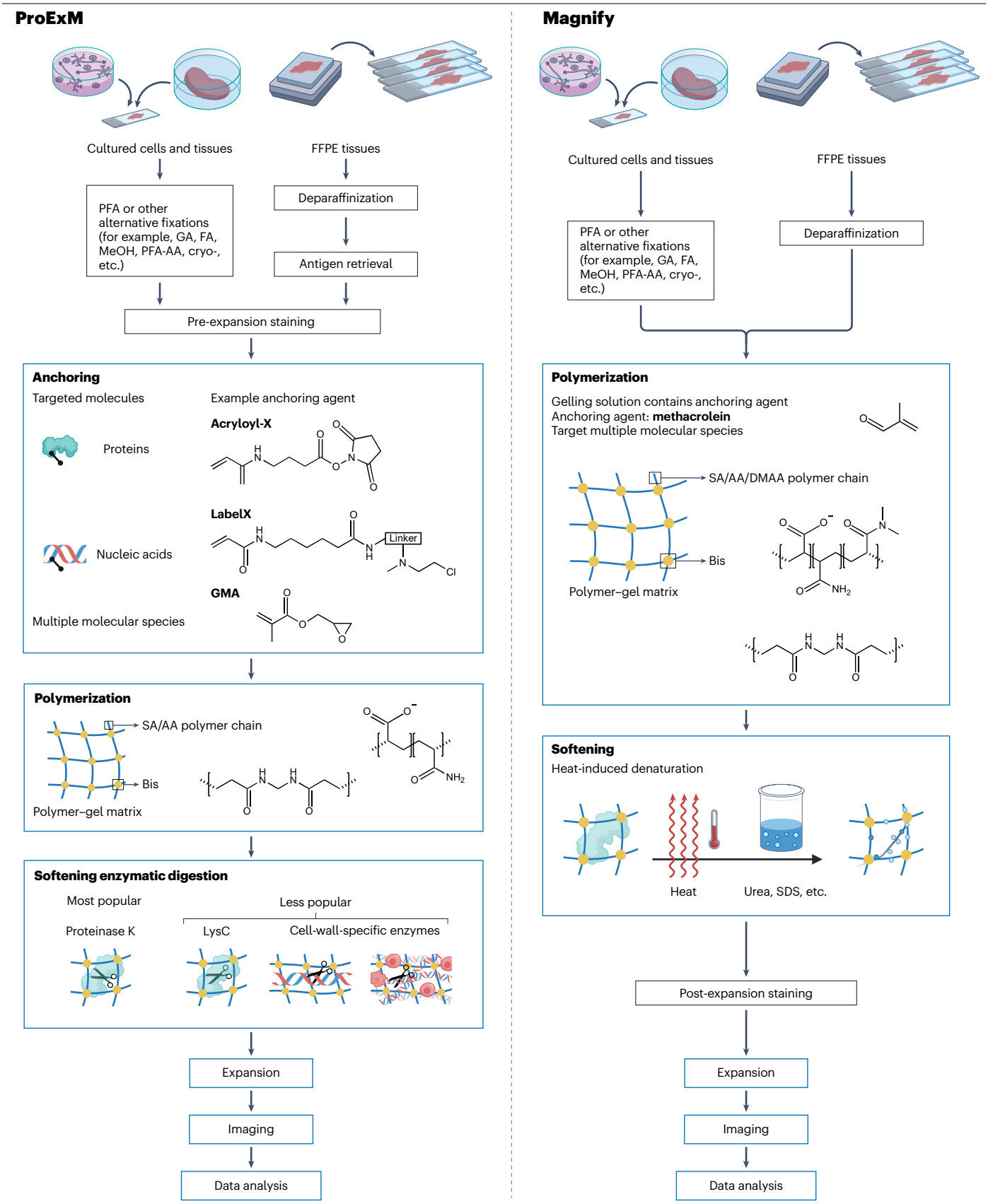
ProExM
Cultured cells and tissues
FFPE tissues
PFA or other alternative fixations (for example, GA, FA, MeOH, PFA-AA, cryo-, etc.)
Deparaffinization
Antigen retrieval
Pre-expansion staining
Anchoring
Targeted molecules
Example anchoring agent
Proteins
Acryloyl-X
Nucleic acids
LabelX
Linker
Cl
GMA
Multiple molecular species
Polymerization
SA/AA polymer chain
Bis
Polymer–gel matrix
NH2
Softening enzymatic digestion
Most popular
Less popular
Proteinase K
LysC
Cell-wall-specific enzymes
Expansion
Imaging
Data analysis
Magnify
Cultured cells and tissues
FFPE tissues
PFA or other alternative fixations (for example, GA, FA, MeOH, PFA-AA, cryo-, etc.)
Deparaffinization
Polymerization
Gelling solution contains anchoring agent
Anchoring agent: methacrolein
Target multiple molecular species
SA/AA/DMAA polymer chain
Bis
Polymer–gel matrix
NH2
Softening
Heat-induced denaturation
Heat
Urea, SDS, etc.
Post-expansion staining
Expansion
Imaging
Data analysis

Fig. 2 | Overview of expansion microscopy workflow, using two pedagogical examples for concreteness. This diagram outlines the modular nature of expansion microscopy (ExM) by comparing the workflows of two representative protocols: protein-retention ExM (proExM)[16] (left) and Magnify[15] (right). The proExM workflow exemplifies a common strategy based on a separate, stand-alone anchoring strategy. This approach is compatible with both pre-expansion and post-expansion staining (with pre-expansion shown here for simplicity). ProExM attaches biomolecules to the gel matrix, which is typically followed by pre-expansion staining. This approach is usually paired with enzymatic digestion (for example, with proteinase K) for the softening step; the Magnify workflow uses a concurrent anchoring strategy in which the anchoring agent is included directly in the polymerization solution. This method is typically paired with heat-induced denaturation for softening, which preserves proteins and is optimized for robust post-expansion staining. These two examples illustrate how different choices for anchoring and softening are linked to the staining strategy, highlighting the modularity that allows researchers to adapt ExM protocols for different experimental goals. AA, acrylamide; Bis, *N*,*N*′-methylenebisacrylamide; DMAA, *N*,*N*-dimethylacrylamide; FA, formaldehyde; FFPE, formalin-fixed paraffin-embedded; GA, glutaraldehyde; GMA, glycidyl methacrylate; MeOH, methanol; PFA, paraformaldehyde; SA, sodium acrylate; SDS, sodium dodecyl sulfate.

brushes[11,38,50,51], coverslips[11,15,38,50–52], parafilm[11,38,50–52] and gel spacers (for example, stacked coverslips[15,38,50–52] or custom-made moulds[53]) used to construct a chamber that controls the thickness of the gel. Key reagents include monomers, such as sodium acrylate (SA) and acrylamide (AA), and crosslinking agents, such as *N*,*N*′-methylenebisacrylamide (Bis), to mediate polymerization. Other key reagents include surfactants and/or protein-digestion enzymes for tissue softening and expansion steps. The specific reagent composition varies depending on the ExM variant used. Protocols such as proExM and Magnify use different anchoring chemistries and polymer networks to optimize biomolecule retention[15,16]. Ensuring the compatibility of these materials with intended staining and imaging techniques is crucial for experimental success.

Sample choices and preprocessing

Different sample types require tailored preprocessing strategies to preserve structural integrity, biomolecule accessibility and compatibility with ExM protocols. Below, commonly used sample types and their corresponding preprocessing requirements are outlined, as well as several alternative options.

Paraformaldehyde-fixed samples. Paraformaldehyde (PFA) fixation is the most widely used for preserving tissue and cellular morphology through protein crosslinking, suitable for general imaging applications. Samples are typically fixed in 4% PFA in phosphate-buffered saline, a method that retains protein organization while maintaining compatibility with most ExM protocols. Other common fixatives, such as glutaraldehyde or methanol, can also be applied before starting ExM (Supplementary Table 1). It should be noted that crosslinking by PFA and other chemical fixatives can mask certain epitopes, potentially reducing the effectiveness of immunolabelling, although this is a problem for all immunostaining not just in ExM[54]. In ultrastructural ExM (U-ExM[21]) and Magnified Analysis of Proteome (MAP[55]), the monomer component AA should be introduced during PFA fixation, to reduce intra-protein and inter-protein crosslinking and to be later incorporated into the hydrogel backbone.

Chemical crosslinking can introduce nanoscale structural artefacts, such as conformational distortions or aggregation, which are a critical consideration when the primary goal is to analyse true-to-life ultrastructure. To address the introduction of artefacts and establish a baseline for structural fidelity, protocols such as U-ExM coupled with cryo-fixation (cryo-ExM) have been developed[56]. These methods use freeze-substitution, which preserves the sample in a near-native, life-like state[57]. However, its requirement for specialized cryo-equipment means that well-optimized PFA and formalin fixation remain the more accessible and dominant standards for the majority of ExM applications. Unfixed samples, by contrast, are not recommended as they can result in incomplete structural preservation[21].

Formalin-fixed paraffin-embedded samples. Formalin-fixed paraffin-embedded (FFPE) samples, commonly used in clinical and archival settings, undergo formalin fixation, dehydration and embedding in paraffin for long-term preservation. Owing to their stability, FFPE samples are valuable for retrospective studies but require specialized preprocessing for ExM. In pathology, deparaffinization is a routine protocol to remove paraffin from FFPE slides, followed by antigen retrieval techniques to reverse excessive crosslinking and expose epitopes, thereby improving protein accessibility in subsequent staining steps[58]. These additional steps are compatible with ExM and enable ExM to be applied effectively to FFPE tissues[14,38].

Ethical considerations. Ethical compliance is a foundational aspect of sample selection. For animal tissues, adherence to institutional guidelines and approval from Ethics Committee, such as the Institutional Animal Care and Use Committee, is required. Researchers should follow the 3R principles: replacement (using alternatives to animals when possible), reduction (minimizing the number of animals used) and refinement (optimizing protocols to reduce animal distress)[59].

Human tissue studies require informed consent, anonymization and compliance with privacy regulations, such as Health Insurance Portability and Accountability Act (HIPAA) in the USA or the General Data Protection Regulation 1 (GDPR) in Europe. FFPE samples, widely used for their archival stability, and fresh or frozen human tissues are valuable resources in translational and clinical research when handled ethically and appropriately documented. It should be noted that research utilizing tissues originally collected for non-research purposes, for example, diagnostic pathology specimens or surgical discards, may qualify for exemptions. Such secondary use exemptions may apply to properly de-identified specimens for research studies that do not require matching clinical information[60]. Researchers should consult with their Institutional Review Board or Ethics Committee to determine exempt qualification before proceeding.

Safety considerations. Sample preparation in ExM involves fixation, anchoring, polymerization and softening steps tailored to the specimen type, often utilizing potentially hazardous chemicals. Organic solvents such as *N*,*N*-dimethylacrylamide (DMAA), and standard fixatives, such as PFA and formaldehyde, are irritants and potential carcinogens; handling these chemicals must be in a fume hood, especially when working with concentrated solutions or solid PFA. Key monomers and crosslinkers used for hydrogel formation, including AA, and Bis, are known neurotoxins and suspected carcinogens, and another monomer, SA, is an irritant and potentially toxic.

Anchoring agents such as Acryloyl-X SE contain reactive groups and should be handled carefully to avoid skin/eye contact and sensitization. Polymerization initiators (for example, ammonium persulfate (APS), *N*,*N*,*N*′,*N*′-tetramethylethylenediamine (TEMED) and 2,2′-azobis[2-(2-imidazolin-2-yl)propane] dihydrochloride (VA-044) can be reactive, irritant, corrosive or toxic, requiring specific handling precautions. Other reagents such as denaturant sodium dodecyl sulfate (SDS) can be an irritant or a sensitizer. Always consult the specific Safety Data Sheet for each chemical before use, work in well-ventilated areas, such as a chemical fume hood for volatile substances or powders, use appropriate personal protective equipment and follow institutional guidelines for proper chemical waste disposal. After complete polymerization and thorough washing to remove unreacted components, the final expanded samples are considered to lack residual toxic monomer components and therefore can be handled safely with standard personal protective equipment such as gloves.

Anchoring strategies in ExM

Anchoring is a core step in ExM, ensuring that biomolecules of interest are retained within the hydrogel matrix throughout the expansion process. Multiple anchoring chemistries exist because macromolecule classes (proteins, nucleic acids, lipids, glycans and small molecules) differ in functional groups, accessibility and tolerance to proteolysis or denaturation and because variants prioritize different goals (universality, retention, ultrastructure and throughput). Protein-amine-reactive *N*- hydroxysuccinimidyl (NHS)-ester anchors (such as Acryloyl-X (AcX[9,16]) and methacrylic acid (MA)-NHS[17]) are simple and broadly compatible with antibodies and fluorescent proteins, enabling robust protein retention in classic/proExM. This anchoring strategy offers simplicity and reproducibility. Click-chemistry frameworks (Click-ExM[61]) add broad molecular reach via metabolic or chemical installation of azide/alkyne handles, affording unified labelling across biomolecule classes and resistance to protease digestion. 'Universal' co-polymerization anchors (such as methacrolein in Magnify[15]) graft diverse biomolecules during gelation, increasing retention including lipids and enabling post-expansion staining. This strategy is beneficial as it allows high retention across classes. However, it requires optimization of monomer composition and softening per tissue type. Fixation-embedded anchoring (for example, MAP[55] and U-ExM[21]) co-grafts proteins by adding AA during formaldehyde fixation, which improves broad antibody compatibility and low distortion, but dependent on careful tuning of fixation and monomer levels[55,62]. Collectively, anchor choice is a trade-off among chemical scope, retention under denaturation or digestion, ease of use and compatibility with specific samples and labelling strategies.

Here, we classify anchoring strategies based on whether the anchoring process occurs concurrently or independently. Most ExM protocols rely on stand-alone anchoring strategies, in which biomolecules are chemically equipped with anchors that are later linked to the hydrogel during polymerization. However, newer approaches can utilize concurrent anchoring during polymerization, an alternative that may streamline workflows (Supplementary Table 1).

ProExM exemplifies a stand-alone anchoring strategy in ExM, relying on Acryloyl-X (acryloyl-6-aminocaproic acid) to anchor proteins. Acryloyl-X, a bifunctional molecule, reacts with primary amines in proteins and equips them with AA groups that crosslink to the hydrogel during polymerization, effectively securing proteins to the matrix[16]. This method offers broad applicability for various sample types, including cultured cells and tissues, and achieves robust protein retention for detailed structural imaging. MA-NHS ExM uses an analogous molecule, MA-NHS ester, for amine-reactive anchoring[17]. Protocols such as MAP[55] and U-ExM[21] incorporate AA during respective formaldehyde fixation. In MAP, AA introduces chemical handles into the sample that participate in radical polymerization during gel embedding[55]. In U-ExM, formaldehyde reacts with amine groups in proteins and with AA to anchor molecules to the hydrogel[21].

These anchoring strategies are, however, limited to proteins and other amine-bearing molecules. To expand the versatility of ExM, specialized anchoring strategies have been developed for specific biomolecular targets. The first nucleic-acid targeting protocol, ExFISH, utilized small-molecule linkers to anchor RNAs. The linker, called LabelX, consists of Label-IT, a commercially available alkylating agent which reacts with the N7 position of guanine bases in RNA molecules, and AcX, which covalently links to the hydrogel[24]. Expansion-assisted iterative fluorescence in situ hybridization (EASI-FISH), which uses Melphalan conjugated to AcX, or MelphaX, anchors RNA molecules in a similar manner[63]. Both methods allow delivery of oligonucleotide probes to perform single-molecule FISH and, if desired, hybridization chain reaction (HCR) for signal amplification of probes bound to single RNA molecules. Transcripts were shown to be well anchored in the hydrogel such that they could withstand sequential rounds of single-molecule FISH. Other methods use acrydite (a vinyl group bearing moiety)-modified FISH probes, which can be incorporated into the polymer hydrogel, and thus can indicate the location of mRNA transcripts that they bind[25,64].

Lipids present a challenge for ExM because they can be washed away by detergents during sample processing and, unlike proteins, they lack some chemical groups (such as primary amines) targeted by standard anchoring chemistries[46]. One challenge, therefore, is to covalently anchor these molecules – or labels attached to them – to the hydrogel network to ensure their retention during expansion[46]. One approach involves metabolic labelling of endogenous lipids in live cells. One such example is lipid ExM, which uses a two-step process[49,65]. First, cells are cultured with a choline analogue containing an alkyne handle (such as propargylcholine). This molecule is metabolically incorporated into native phospholipids such as phosphatidylcholine[49]. After fixation, the alkyne handle is then used to covalently link the lipid to the hydrogel through a click chemistry reaction, via a trifunctional molecule that binds to the alkyne (via an azide group) and contains a polymerizable group, as well as a fluorophore. A second strategy utilizes exogenous lipophilic probes that are designed to insert themselves into cellular membranes and that bear moieties that can, at a later step, incorporate both a fluorophore for visualization and a chemical group for anchoring to the hydrogel. For instance, ultrastructural membrane ExM (umExM) uses a custom-made probe called pGk13a (palmitoyl-glycine-(D-lysine)13-azide)[66]. This probe has a lipid tail (palmitoyl) that inserts into membranes, while its chain of lysine residues provides primary amines for covalent anchoring to the hydrogel via an Acryloyl-X-like linker. The probe also includes a terminal azide group, which serves as a chemical handle to attach a fluorophore via click chemistry[66]. To better preserve membrane integrity during fixation, the umExM protocol also incorporates 0.5% calcium chloride into the fixative solution, and the entire process is conducted at cold temperatures (4 °C) until molecules are locked in place. With this strategy, umExM was reported to enable dense, continuous labelling of a wide range of structures, including plasma membranes, mitochondrial membranes, the nuclear envelope, ciliary membranes, myelin sheaths and extracellular vesicles[66].

Several approaches have been reported for their compatibility to anchor more than one class of biomolecule[15,28,44]. Magnify introduces a combination of anchoring and polymerization into a single experimental step. The method uses methacrolein, a broad-spectrum anchoring reagent that reacts with a wide range of biomolecules — including proteins, nucleic acids and lipids — during hydrogel synthesis[15,44]. Protein retention in Magnify-processed mouse brains and kidney FFPE tissue was reported to be 6.3-fold and 4.8-fold higher than proExM-processed tissues, respectively, in large part owing to the improved anchoring. Up to 93% of lipid content in the mouse brain was retained when comparing fluorescence intensity of the lipophilic stain DiIC18(5) solid (1,1′-dioctadecyl-3,3,3′,3′-tetramethylindodicarbocyanine and 4-chlorobenzenesulfonate salt) pre-Magnify and post-Magnify processing. This concurrent anchoring strategy streamlines the protocol by integrating anchoring directly into the polymerization process, while retaining diverse biomolecular classes. For the similar purpose of eliminating the need for a separate anchoring step, united ExM[28], which uses a multifunctional anchor that contains an acrylate group and an epoxide group (glycidyl methacrylate), equips proteins and RNAs, and potentially other biomolecules, with anchors in a single step. Epoxide-anchored expanded tissues were shown to be compatible with proExM[16], ExFISH[24] and expansion sequencing (ExSeq[23], the combination of ExM and fluorescent in situ sequencing of RNA).

Polymerization strategies in ExM

Hydrogel polymerization is a critical step for incorporating biological samples within the polymer network. SA/AA/Bis gels with an APS inhibitor and TEMED accelerator are well established, reproducible systems and are a recommended starting point to validate antibodies and workflows, offering predictable expansion factor and good isotropy. For SA/AA/Bis gels with or without low percentage of DMAA (proExM[16], U-ExM[21], MAP[55] and Magnify[15]) and AA/Bis only (ZOOM[67]), properly sealing the gel chamber is sufficient to limit oxygen access by minimizing exposure to atmosphere, with no need for active oxygen removal. By contrast, gel formulae with high percentages of DMAA (such as ×10^{10} or 20-fold ExM (20× ExM[11])) require careful management of oxygen removal (by nitrogen bubbling or purging) to avoid inhibition and to ensure uniform polymerization and reproducible expansion factors.

To further guide selection, Table 1 provides a comparative overview of monomers, crosslinkers and initiators across major ExM formulas, including their effects on polymer quality and expansion isotropy. For example, APS/TEMED offers fast, room-temperature initiation but may lead to premature polymerization if not controlled; VA-044 enables slower, uniform gelation at ~37 °C, improving isotropy in thick tissues but requiring temperature control and potentially generating gas bubbles of various sizes in the gel[68], causing scattering in some imaging conditions.

Table 1 | Comparative overview of gel polymerization strategies in major expansion microscopy variants

ExM variant/group	Monomer composition	Crosslinker	Initiator/accelerator	Degas?	Duration	Comment
Classic (proExM[16], Click-ExM[61], TREx[19] and derivatives)	SA + AA	Bis	APS/TEMED	No	37°C for 2 h	Robust starting point; predictable ~4–10× expansion
Thermal-initiated (MAP[55], eMAP[62], and derivatives)	SA + AA (high AA in MAP/eMAP)	Bis	VA-044 (thermal)	No	4 °C for 8–12 h and then 37°C for 1–2 h	Applied for whole-organ expansion; ~4× expansion; temperature control needed; may generate bubbles
High-swelling DMAA-based (×10^{10}, 20× ExM[11])	High DMAA + SA	Self-crosslinking by DMAA	KPS/TEMED or APS/TEMED	Yes	RT for 6–24 h	High resolution (~10–20×); oxygen-sensitive, requires N_2 purging
Iterative/high expansion (iExM[12], ExR[71], pan-ExM[73])	SA/AA (initial); varies in iterations	Cleavable crosslinker or Bis	APS/TEMED	No	4 °C for 30 min to overnight (or RT for 15 min in pan-ExM) and then 37°C for 1.5–3 h	Cumulative ~13–24×; complex and longer processing time
ZOOM[67]/high-AA hydrolysis approaches	High AA (post-hydrolysis)	Low Bis	APS/TEMED	No	40 min to 3 h at RT	Tunable expansion factor up to ~8× via hydrolysis; requires hydrolysis control
Tetra-gel[198]/tetra-PEG	Tetrahedral PEG	Inherent to monomers	Click reactions (non-radical)	Yes	RT for 2 h	Designed for isotropic, homogeneous hydrogel networks; needs specialized reagents
Magnify[15]/MicroMagnify[44]	Low DMAA + high SA/AA	Bis	APS/TEMED	No	4 °C for 30 min and then 37°C overnight	~11× for FFPE/pathogens; broad compatibility; optimize per tissue
Photoinitiated group (PhotoExM[212])	SA + AA	PEGdiAcM	LAP (photoinitiator, UV)	Yes	15 min at RT and then irradiated for 70 s	~4× with clearance; low-temperature gelation; UV penetration limited in thick tissues; uneven illumination challenges

AA, acrylamide; APS, ammonium persulfate; Bis, *N*,*N*′-methylenebisacrylamide; DMAA, *N*,*N*-dimethylacrylamide; eMAP, Epitope-preserving Magnified Analysis of Proteome; ExM, expansion microscopy; ExR, expansion revealing; FFPE, formalin-fixed paraffin-embedded; iExM, iterative expansion microscopy; KPS, potassium persulfate; LAP, lithium phenyl-2,4,6-trimethylbenzoylphosphinate; MAP, Magnified Analysis of Proteome; PEG, polyethylene glycol; PEGdiAcM, PEG–diacrylamide; proExM, protein-retention ExM; RT, room temperature; SA, sodium acrylate; TEMED, tetramethylethylenediamine; TREx, tenfold robust ExM; UV, ultraviolet.

Staining strategies in ExM

Staining strategies in ExM are critical to its success and can be categorized into two main approaches: pre-expansion and post-expansion staining. Each approach is tailored to specific methodological requirements and sample characteristics.

Pre-expansion staining. Pre-expansion staining, in which samples are labelled with fluorescent probes before hydrogel embedding and expansion, is a widely used strategy in many ExM protocols, exemplified by the classical proExM method[16]. This strategy is usually coupled with proteinase K-based softening methods, as antibodies are in part preserved during proteinase K digestion. Researchers can apply previously validated antibody markers, using standard immunofluorescence procedures, and expect staining outcomes similar to their previous tissue staining outcomes[11,12]. Furthermore, this approach effectively preserves the signal from many genetically encoded fluorophores. For instance, green fluorescent protein (GFP) has been reported to exhibit good resistance to hydrogel polymerization and proteinase K-based softening, retaining ~65% of its fluorescence after expansion[16,69].

However, a key consideration for this approach is the potential for signal loss during processing. This can occur from two main sources: damage to the fluorescent dyes or fluorescent proteins themselves by free radicals generated during gel polymerization, and partial degradation of fluorophore-conjugated antibodies and fluorescent proteins during enzymatic softening. Susceptibility to this degradation varies substantially among different types of fluorescent dye and fluorescent protein. For example, it was reported that some dyes, including Alexa Fluor 488, Alexa Fluor 546 and ATTO 647N, retained more than 50% of their signal strength through the proExM process, whereas others such as Alexa Fluor 647 showed much lower retention[16]. The same study found that some common fluorescent proteins, including GFP, yellow fluorescent protein, tdTomato and mCherry, retained more than 50% of their initial fluorescence after the proExM protocol, whereas the near-infrared fluorescent protein iRFP was less stable (although see ref. 70 for an experiment set that showed lesser performance of red fluorescent protein). The fluorophores summarized in Supplementary Table 3 are specifically validated for their ability to survive the complete pre-expansion staining workflow (for example, gel polymerization and proteinase K digestion in proExM); some common dyes, such as Alexa Fluor 647, show poor retention in this specific context. This limitation, however, generally does not apply to post-expansion staining. In a post-expansion workflow, the dye is applied after all harsh processing steps, so nearly any modern, bright fluorescent dye can be used successfully, including those that fail pre-expansion. Despite these considerations, pre-expansion staining remains a common and reliable approach for many applications when leveraging well-validated antibodies or existing fluorescent protein expression in a biological system.

Post-expansion staining. Post-expansion staining, which involves labelling the sample after physical expansion, was a critical methodological innovation in ExM. The concept was first introduced by the foundational proExM[16] and MAP[21] protocols, which demonstrated that antibodies could be applied after processing. This post-expansion paradigm was quickly optimized by protocols such as U-ExM[21], expansion revealing (ExR)[71], decrowding expansion pathology (dExPath)[39] and Magnify[15]. Unlike pre-expansion staining, this approach is incompatible with nonspecific protein-cleaving softening methods such as those using proteinase K. Instead, post-expansion staining typically requires that the hydrogel-embedded specimen be processed using heat-induced denaturation, often with solutions containing surfactants and denaturants, such as SDS and/or urea. Post-expansion staining offers several key advantages. First, because the staining occurs after hydrogel polymerization, the fluorophores are not exposed to potential degradation from free radicals generated during polymerization[15]. Second, the expansion process effectively decrowds densely packed proteins, which can enhance antibody accessibility to previously sterically hindered epitopes[39]. This often results in improved labelling density and can yield stronger signals for the same protein targets compared with pre-expansion staining[15,39,71]. A high success rate for antibody compatibility has been reported for this approach; for example, the original MAP protocol found that ~82% of the antibodies tested were effective for post-expansion staining[55]. The improved access provided by decrowding can also reveal new staining patterns that were not visible in unexpanded tissues, effectively converting invisible targets into visible ones. For instance, the ExR protocol demonstrated that post-expansion staining could unmask synaptic proteins within intact brain circuits that were previously inaccessible to antibodies, allowing for the discovery of novel nanostructures, such as the nanocolumnar organization of synaptic calcium channels[71]. Similarly, dExPath applied to human glioma specimens revealed previously unobserved, disease marker-positive cell populations by improving antibody access to epitopes within densely packed tumour cells[39]. Careful controls may be required to ensure that such patterns are not caused by nonspecific staining, such as comparison with known gene expression data, use of multiple antibodies against the target or standard antibody controls including blocking peptides or knockouts; the choice of control will depend on the specific scientific question.

Pan-protein staining. Pan-molecular staining enables the visualization of broad classes of biomolecules (all proteins) without specific probes, producing EM-like structural contrast over thick 3D specimens. Pioneered by methods such as Fluorescent Labelling of Abundant Reactive Entities (FLARE)[72] and pan-ExM[73], this approach typically uses small, reactive fluorescent dyes (most commonly NHS esters) applied after expansion. These dyes covalently bind to abundant chemical groups, such as primary amines on lysine residues on most proteins. This strategy has two powerful benefits. First, it is a good starting point for beginners; the resulting bright, high-intensity signal acts as a vital counterstain, making it much easier to navigate the transparent gel and locate sparser, antibody-labelled targets. Second, its widespread adoption underscores its power as a discovery tool, enabling the resolution of fine ultrastructural details — from the ninefold symmetry of cilia and nuclear pore architecture to individual protein shapes[74] — supporting applications across diverse and complex systems, including protocols for connectomics (LICONN[75]), pathogens (MicroMagnify[44] and U-ExM for yeasts), whole mouse bodies (whole-body ExM[13]) and plant roots[76–78].

Choice of softening methods

The softening step in ExM is pivotal to ensure uniform and isotropic expansion. Primarily, softening is used to break down intermolecular interactions between molecules, thereby sufficiently disrupting cell or tissue rigidity while preserving anchored biomolecules and maintaining their relative spatial organization within samples. Depending on the tissue type, organism and biological question, selecting the appropriate softening method requires careful consideration, as both insufficient and excessive softening can compromise the success of the experiment. In this section, the softening methods are categorized

and discussed as two principal approaches: enzymatic digestion and heat-induced denaturation.

Enzymatic digestion. Enzymatic digestion is a widely used method in ExM. Proteinase K (ProK) is the most used enzyme owing to its broad substrate specificity and ability to fragment proteins, making it effective for mechanically softening cell and tissue samples. It is the standard choice for ExM protocols that use pre-expansion staining, as the harsh enzymatic digestion destroys most protein epitopes, precluding post-expansion antibody labelling, but antibodies, and many genetically encoded fluorophores, survive this process at least in part. As ProK digestion does not target RNA or DNA, it is compatible with nucleic acid anchoring protocols such as those used in ExFISH[24], ExSeq[23] and expansion spatial transcriptomics (Ex-ST[27], ExM combined with spatial transcriptomics as performed in commercial platforms such as Visium, which slide-captures polyadenylated RNAs). For applications aiming to preserve some epitopes for post-expansion immunostaining, more specific proteases such as LysC and trypsin have been explored as gentler alternatives to the broad-spectrum ProK[11,16]. Unlike ProK, which cleaves proteins in many locations, these enzymes are more specific. Trypsin, for example, only cuts a protein chain after specific amino acids (lysine and arginine), whereas LysC is even more specific, cutting only after lysine residues[79–81]. This high specificity means that they cleave proteins much less frequently, resulting in fewer and larger protein fragments. The rationale is that by keeping larger fragments intact, there is a greater chance of preserving epitopes for subsequent antibody binding, making them potentially suitable for some post-expansion staining applications.

Many biological specimens contain structures, such as extracellular matrices (ECMs) or rigid cell walls, that require specialized enzymatic treatments in addition to standard softening methods to achieve uniform softening and isotropic expansion. For animal tissues rich in connective proteins, the ECM composed of collagen, elastin and fibronectin can physically resist expansion. Connective and structural tissues such as bone, cartilage, muscles, tendons and protective outer layers in whole organs or whole organisms may not be fully digested by proK treatment. Therefore, protocols designed for tough tissues or whole organisms, such as expansion of *Caenorhabditis elegans* (ExCel)[82], tissue ultrastructure ExM (TissUExM)[83] and whole-body ExM[13], incorporate an additional collagenase digestion step, and other specialized steps to soften tough biomaterials of interest, to ensure uniform expansion. ExCel used collagenase type VII (enzyme that breaks down collagen types I and III in connective tissues) to thoroughly digest the tough cuticle layer in *C. elegans* and showed improved isotropic expansion compared with no-collagenase treatment[82]. Furthermore, it was reported that the addition of collagenase VII helped digest the developing skeleton in zebrafish embryos in TissUExM[83]. Additionally, hydrogel-embedded mouse embryos could be digested with cycles of proK and collagenase, in addition to EDTA treatment to decalcify bone, in the whole-body ExM protocol[13]. The combination of proK and a collagenase mixture, and decalcification, helped digest tissues such as bone, cartilage and muscle[13].

Similarly, organisms with rigid cell walls require specialized enzymes to degrade these protective barriers to ensure uniform softening and isotropic expansion. The choice of enzyme is dictated by the specific composition of the cell wall, which varies across different species. For plants, whose walls can contain cellulose, hemicellulose and pectin, a cocktail of enzymes including driselase[76,77], cellulase[77,78], macerozyme[77,78] and/or pectolyase[77] can help with digestion. In fungi such as yeast, the cell wall can contain polysaccharides (such as glucans and chitin) and proteins and can be digested using enzymes such as zymolyase or lyticase[84–87]. For bacteria, one structural component can be peptidoglycan[88,89]. To degrade this layer and prevent distortion during expansion, ExM protocols for both Gram-positive and Gram-negative bacteria can use enzymes such as lysozyme and mutanolysin[44,46–48,90,91]. In general, if the composition of the mechanically tough part of species, cell or tissue is known, and if there is a targeted way of softening it, it is often straightforward to incorporate that as part of the softening step of ExM.

Heat-induced denaturation. Heat-induced denaturation offers an alternative to enzymatic digestion for softening gelled tissues and cells and is the standard for most modern protocols that require post-expansion immunostaining. This approach relies on elevated temperatures (70–121 °C) in the presence of chemical denaturants and surfactants such as SDS[11,15,92], and reducing agents such as urea[15], β-mercaptoethanol[39], dithiothreitol[11] and sodium sulfite[55,62], to facilitate unfolding of protein structures and loosen the tissue structure[93]. Compared with ProK digestion, this approach allows for proteins to be retained in the gel without being nonspecifically digested, enabling post-expansion immunostaining.

The specific conditions are tuned to the sample type. For standard PFA-fixed cells or tissues, a common condition is 95 °C for 1 h in a denaturation buffer containing a low concentration of SDS (less than 10%) and a reducing agent (such as dithiothreitol)[11,71]. For more challenging, heavily crosslinked clinical FFPE tissues and stronger decrowding conditions, for example, high temperature and high surfactant concentration, are required. For example, dExPath uses an autoclave (121 °C) with 20% SDS, EDTA and the reducing agent β-mercaptoethanol to reduce non-covalent inter-protein and intra-protein interactions and to cleave disulfide bonds between proteins in FFPE-preserved brain tissues[39]. A similar strategy has been applied in high-expansion-factor protocols such as Magnify, in which methacrolein-anchored tissues (PFA-fixed cells or brain samples, FFPE tissues and multiple organs) undergo heat denaturation in a buffer with 10% SDS, 8 M urea and 25 mM EDTA at 80 °C for 36 h (ref. 15). This principle was further adapted in MicroMagnify, which couples a similar heat-induced denaturation step with an additional cell-wall-digesting enzymatic cocktail[44]. Protocols such as MAP[55], Epitope-preserving MAP (eMAP)[62] and U-ExM[21] use a fixation step using formaldehyde and AA to reduce inter-protein and intra-protein crosslinks, making subsequent heat-based softening highly compatible with antibody epitopes; U-ExM uses a similar approach but with reduced formaldehyde-AA concentrations for improved ultrastructure preservation.

Heat-induced denaturation is highly effective for post-expansion immunostaining against most protein targets[55,62], but researchers should be aware of specific considerations for certain types of applications. For example, in experiments focused on RNA imaging, the high temperature can lead to hydrolysis of RNA[94], rendering protocols such as ExFISH[24] or ExSeq[23] incompatible or diminished in signal quality. Additionally, although this approach has shown to preserve the linear amino acid sequences that form many epitopes, the denaturation process can alter the 3D structure of proteins. This means that conformational epitopes (those dependent on the folded shape of the protein) may be lost. Consequently, antibodies that bind to epitopes on denatured proteins, such as those used for western blot, are preferred candidates for post-expansion staining, whereas antibodies known to target conformational epitopes may not be suitable.

Results

Data acquisition in ExM

Wide-field and confocal fluorescence microscopy. Wide-field and confocal fluorescence microscopes are widely accessible, fast and compatible with common fluorescent dyes and labelling techniques, making them well suited for visualizing expanded specimens. Wide-field microscopy is often used for rapid, 2D imaging, whereas confocal microscopy provides the optical sectioning necessary for detailed 3D structural imaging[15,16,23,45]. The point-scanning confocal is a robust workhorse for acquiring high-resolution *Z*-stacks. To enhance the resolution and signal-to-noise ratio (SNR) of these systems, they are often combined with image-scanning microscopy (ISM) detection, such as the Zeiss Airyscan, or equivalent technologies, such as Nikon AX R with NSPARC, Olympus (now Evident) FV3000 with TruResolution or FV-OSR (Optical Super Resolution) or Leica STELLARIS. ISM provides a 1.5–1.7× resolution gain over standard confocal imaging, making it a practical and widely used approach for ExM[95]. For applications prioritizing throughput and large-volume acquisition, spinning disc confocal microscopes (such as Nikon with Yokogawa CSU-W1, Andor Dragonfly) offer a valuable alternative. Although standard spinning disc systems typically yield diffraction-limited resolution (~250 nm) – slightly lower than optimized ISM set-ups – they utilize parallelized pinhole scanning to achieve superior acquisition speeds, often one order of magnitude faster than point-scanning systems[96,97].

Choice of objectives. For the imaging step, although a standard confocal or wide-field microscope is sufficient, optimizing for thick, expanded samples requires specific hardware considerations. Because the expanded hydrogel is ~99% water (with a refractive index, RI ~1.33), standard high-numerical aperture (NA) oil immersion objectives (RI ~1.52) will suffer from severe spherical aberrations when focusing deep into the sample. Therefore, the use of a long working distance (LWD) water-immersion objective is a critical and highly recommended practice. These objectives are designed to match the RI of the sample, minimizing aberrations. They also offer a substantially longer working distance to accommodate the thick, expanded gel. For example, a typical 40× high-NA oil objective may have a working distance of only ~0.15–0.21 mm, which is insufficient for imaging deep into a multi-millimetre thick gel. By contrast, a comparable 40× water-immersion objective can offer a working distance of ~0.6 mm or more – a threefold to fourfold increase. This extended working distance is essential for maintaining focus and achieving high resolution deep within thick, expanded specimens.

Light-sheet fluorescence microscopy. Light-sheet fluorescence microscopy (LSFM) is increasingly used for ExM, for large samples and correspondingly large volumetric datasets. By illuminating the sample with a thin sheet of light perpendicular to the detection axis, LSFM offers very rapid acquisition speeds and reduced photobleaching compared with point-scanning confocal microscopy, making it well suited for imaging the large, transparent volumes possible with ExM samples[70,98,99]. One potential concern is the poorer resolution of some light-sheet systems compared with confocal, especially when very large volumes are being imaged, and correspondingly LWSs are being used. The core consideration is how to balance imaging speed, resolution and volume acquired, to meet the needs of the scientific question at hand.

Optimizing imaging protocols. Achieving good image quality in ExM requires careful calibration of microscope settings to balance resolution, SNR and photobleaching[100]. A critical factor is the choice of microscope objective, as its properties – NA, working distance and immersion medium – directly dictate the achievable optical resolution and the ability to image deep into the expanded sample. The NA determines the light-gathering ability and ultimate resolution of the objective; a higher NA yields better optical resolution. Water-immersion objectives are strongly preferred for ExM. First, they are often designed for longer working distances compared with high-NA oil objectives, which helps with focusing deep into a physically thick, expanded hydrogel. Second, the immersion medium (water) closely matches the RI of the expanded gel, which is mostly water. This RI matching is crucial for minimizing spherical aberrations – optical artefacts that can severely degrade image quality and resolution when imaging deep into the sample.

Once an objective is chosen, the illumination power (from a laser or light-emitting diode or other light sources) should be adjusted to provide sufficient fluorescence intensity without over-illuminating the sample, as excess energy can lead to photobleaching. Similarly, camera exposure time or pixel dwell time must be carefully managed; prolonged exposure can enhance signal but also could increase photobleaching. Given the volumetric dilution of fluorophore by the cube of the expansion factor, and the potential for fluorophore loss, label quality should be as good as possible, in addition to the optical considerations mentioned earlier[16,50,101]. For 3D imaging, the choice of *Z*-stack interval is crucial[102]. To accurately capture the data, the interval should be smaller than the optical section thickness of the microscope, adhering to the Nyquist sampling criterion[103]. This ensures that the final dataset faithfully represents the expanded sample, especially in regions with densely packed labelled structures.

The effective resolution in ExM is determined by the interplay between the physical expansion factor and the optical resolution of the microscope, typically ranging from ~15 nm to 75 nm for common protocols (4–20× expansion) on standard confocals (~300 nm optical limit). For instance, a 4× expansion yields ~75 nm effective resolution, whereas 10–20× expansion can achieve ~15–30 nm, although practical limits also depend on labelling density and linkage error (fluorophore size relative to target). Although not yet ubiquitous, combining ExM with established super-resolution techniques, such as STED[21,92,104–107], SIM (structured illumination microscopy)[108–112], SMLM (stochastic optical reconstruction microscopy (STORM) and photoactivated localization microscopy)[113–117], super-resolution radial fluctuations[41] and SOFI (super-resolution optical fluctuation imaging)[15,107], has become a useful strategy to further enhance resolution, often by 2–10× beyond ExM combined with diffraction-limited microscopes, enabling sub-10 nm imaging in diverse samples (Table 2). For example, ExM + SIM (ExSIM[109,110]) at ~3.5× expansion routinely achieves ~30 nm lateral and ~75 nm axial resolution with low (~2%) distortion, whereas ExM + STED (ExSTED[104]) at ~4× can reach sub-10 nm lateral resolution in microtubules or spectrin rings – and down to <9 nm with amplification – although photobleaching and labelling density remain constraints. ExM combined with SMLM – often with post-labelling to minimize linkage error – achieves ~10 nm resolution at ~2.5–4× expansion[115], with iterative variants (>20×) approaching molecular-scale precision. These hybrids leverage physical decrowding of ExM to improve probe access and reduce demands on super-resolution hardware (for example, lower STED powers), making them suitable for thick tissues (see Table 2 for more examples).

Navigating expanded samples. Expanded samples are highly transparent, with an RI close to that of water[16,118,119]. Although this facilitates

Table 2 | Advances involving combining expansion microscopy with other techniques

Technique	Expansion factor	Resolution	Note
ExM combined with super-resolution imaging techniques			
ExM + STED[21,92,104–107]	~4–10×	~20–40 nm	Combines ExM with STED to achieve fine-scale nanoscale resolution
ExM + SIM[108–112]	~3–4.2×	~30 nm	Hybrid ExM–SIM methods for fine-scale sub-diffraction limit resolution
ExM + SMLM (for example, STORM and PALM, etc.)[113–117]	~2.37–4×	~15–25 nm	Combines ExM with localization microscopy for precise molecule-level imaging
ExM + SRRF[41] ExM + SOFI[15,107]	~4.5× ~4× (ExSOFI)–11× (Magnify)	Up to 15 nm	Combines ExM with SRRF or SOFI fluctuation analysis
ONE[74]	~10×	~1 nm	Combines ×10 ExM with SRRF fluctuation analysis to resolve individual protein shapes
ExM combined with vibrational imaging			
MAGNIFIERS[195]	~7.2×	~41 nm	Enables super-resolution vibrational imaging with ExM
VISTA[196,197]	~4×	~78 nm	Combines vibrational signals with ExM for high-resolution, label-free imaging
ExM combined with spatial omics techniques			
ExSeq[23]	~3.3–3.5×	~70–100 nm	Integrates ExM with in situ sequencing for spatially resolved transcriptomics
EASI-FISH[63]	~2–3×	~100 nm	Combines ExM with FISH and deep-learning segmentation for thick tissue spatial organization analysis
Ex-ST[27]	~2.5×	20 µm	Combines ExM with spatially resolved transcriptomics assay V for high-resolution spatial transcriptomics
Expansion MERFISH[25]	~2×	~174 nm	Combines ExM with MERFISH for high-throughput spatial transcriptomics
ExM combined with mass spectrometry imaging			
ExM + LC–MS/MS[202] ProteomEx[203]	Up to 3×	~330 µm ~160 µm (ProteomEx)	Integrates ExM with LC–MS/MS for spatial proteomics analysis
GAMSI[205]	Up to 6×	~880 nm	Combines ExM and MALDI mass spectrometry imaging for sub-micrometre spatial analysis
TEMI[204]	~3.5×	~3 µm	Combines ExM and LC–MS/MS for high-resolution spatial multi-omics profiling

EASI-FISH, expansion-assisted iterative fluorescence in situ hybridization; ExM, expansion microscopy; ExSeq, expansion sequencing; Ex-ST, expansion spatial transcriptomics; GAMSI, gel-assisted mass spectrometry imaging; LC, liquid chromatography; MALDI, matrix-assisted laser desorption; MERFISH, multiplexed error-robust FISH; MS, mass spectrometry; ONE, one-step nanoscale expansion; PALM, photoactivated localization microscopy; SIM, structured illumination microscopy; SMLM, single-molecule localization microscopy; SOFI, super-resolution optical fluctuation imaging; SRRF, super-resolution radial fluctuation; STED, stimulated emission depletion; STORM, stochastic optical reconstruction microscopy; TEMI, tissue-expansion mass spectrometry.

light-sheet imaging, even to the point of not requiring adaptive optics in some cases[70], this can present challenges in navigating the sample and locating specific regions of interest. Strategic sample preparation can mitigate these difficulties. For example, cutting the gel (at a site outside the biospecimen itself), to result in an asymmetric gel shape, can allow for quick orientation[98]. Another useful technique is to acquire a low-magnification map of the whole specimen, before zooming in with a higher magnification[9,118]. This can be useful for calculating the expansion factor, by dividing the size of a landmark taken with low magnification, pre-expansion versus post-expansion.

Additional considerations for high-resolution imaging. Expanded samples often require specific mounting strategies to ensure stability during imaging[119]. Because the expanded hydrogel is composed of more than 99% water, it is more physically delicate than the original specimen (although with proper handling, it can be reasonably robust), and because of its neutral buoyancy, it can drift in the imaging dish during long acquisitions. This movement, even if subtle, can introduce motion artefacts in the image. Most users will thus want to firmly immobilize the gel before imaging[50]. One effective method is to embed the expanded ExM gel within a secondary, more rigid gel. This typically involves placing the expanded sample in the imaging dish and then carefully surrounding it with a low-concentration (~0.5–1%) low-melting-point agarose gel[9]. Once solidified, the agarose provides a stable matrix that holds the delicate ExM gel in place. Another widely used approach[21] is to coat the glass surface of the imaging dish or coverslip with an adhesive molecule, such as poly-D-lysine. The surface is treated with poly-D-lysine solution and allowed to dry, creating a positively charged layer. The negatively charged expanded hydrogel can then be carefully placed onto this coated surface, where it will adhere, preventing it from drifting during imaging. Owing to the large physical size of expanded samples, an entire region of interest may not fit within a single microscope field of view. In such cases, acquiring multiple adjacent images (tiling) and computationally combining them (stitching) can help to create a single, seamless, high-resolution image of the entire area.

Computational tools for data analysis

The computational analysis of data from ExM experiments is generally analogous to that for data acquired from conventional diffraction-limited 3D fluorescence microscopy. The workflow typically involves stages such as stitching and assembly, image preprocessing (background subtraction and denoising), 3D visualization, segmentation and tracing (as needed) and quantitative analysis (as determined by the scientific question at hand). All spatial measurements must be scaled by the determined expansion factor to ensure that reported dimensions reflect true biological scale. Although imaging large, expanded volumes can generate substantial datasets, particularly when using high-speed methods such as light-sheet microscopy, the analytical tools and pipelines are often similar in approach to those that researchers would use for other volumetric imaging data[120]. Effectively handling of these datasets may require researchers to utilize multiple software packages specialized for various tasks.

Image preprocessing and visualization. A common first step in ExM data analysis involves image preprocessing. Many routine tasks, such as background subtraction, denoising and histogram scaling, can be performed using widely available open-source software such as Fiji (ImageJ). Available plugins allow researchers to perform functions such as stitching overlapping image tiles[121]. All image processing steps should be disclosed in publication and consider biological context to avoid introducing artefacts or removing relevant signals. Furthermore, for analyses specific to ExM, such as quantifying spatial distortion when a new ExM protocol is being invented[9,19] or performing fluctuation-based super-resolution imaging (for example, SOFI[15]), research groups have developed custom scripts. These tools are often written in MATLAB or Python and are frequently deposited in public repositories such as GitHub, allowing other researchers to download and adapt them for their own use[18,36,61,74].

During preprocessing, initial checks for isotropy — the uniform expansion across dimensions — can be integrated into data assembly workflows to flag potential issues early. For instance, simple landmark-based comparisons in Fiji can estimate local expansion factors and identify potential cracks that suggest insufficient softening or other issues upstream. If anisotropy is detected (via uneven scaling), re-optimization of softening or gelation steps may be required before final analysis.

For visualization tasks, including generating 3D renderings, sometimes software accompanying the microscope system itself (such as Nikon Elements) may be relevant. For researchers requiring more advanced rendering options or quantitative analyses, such as object segmentation and measuring spatial relationships, plugins for open-source packages, custom open-source software and commercial software (such as Imaris) can offer capabilities and user-friendly interfaces for such tasks[108,122].

Beyond these general-purpose tools, several plugins and stand-alone software packages have been developed to address challenges specific to large-scale datasets obtainable via ExM. For example, the Fiji plugin BigStitcher[120,123] may be useful for reconstructing large datasets by stitching overlapping image tiles, deconvolving signals and registering image series. Other tools may address issues such as sample drift, such as 3D-Aligner[124] and ExM studio[125]. Such specialized tools may help with projects involving very large, multi-tile datasets or when trying to correct for motion artefacts during long imaging sessions.

The authors of this Primer have not hands-on tested all these tools — a caveat that holds for many of the wet laboratory procedures as well — so we recommend that researchers evaluate their specific utility and performance for their own experimental context.

Applications

ExM has enabled discoveries across a wide range of biological fields by providing nanoscale resolution on conventional microscopes. The building blocks of life, biomolecules and their relative organization and the distances over which they interact are nanoscale. The rapid adoption of ExM over the past decade to answer biological questions has unlocked many discoveries by allowing researchers to identify, and localize, biomolecules in their specimens.

Applications in cellular and structural biology

The inner workings of a cell are orchestrated by biomolecules, often organized in organelles or other structural compartments with nanoscale organization. ExM makes these structures accessible to conventional fluorescence imaging and enables new insights into fundamental biological processes.

Molecular organization of nuclear components. Inside the cell nucleus, the eukaryotic genome is compacted into chromatin, a complex of DNA and proteins. This organization is hierarchical, starting from the 10-nm nucleosome ('beads-on-a-string'), which folds into complex higher-order structures that ultimately form micrometre-scale chromosome territories[126]. The way chromatin is organized regulates which genes are turned on or off, often through chemical modifications to histone proteins that act like a regulatory code[127–129]. Although sequencing-based assays can identify which histone modifications are present across the genome, they do not reveal their physical, spatial arrangement along the chromatin fibre. ExM helps to bridge this gap. For example, an ExM method for epigenetics was developed to spatially map multiple histone modification patterns on individual genes within single cells[30]. This approach made it possible to directly visualize how different epigenetic marks were arranged on both housekeeping and developmentally regulated genes, revealing cell-to-cell variability in these nanoscale patterns. To study the transcriptional machinery itself, ChromExM was developed and applied to zygotic genome activation, in which embryos are reprogrammed to become zygotes. ChromExM was used to map transcription factors, nucleosomes and RNA polymerase II, visualizing the transcriptional machinery (Fig. 3a). The images produced resulted in a new hypothesis that they call the 'kiss and kick' model, in which certain DNA contacts (enhancers and promoters) are transient, and transcription terminates the contact[31,130]. More recently, ExM with in situ genome sequencing has been used to connect abnormalities in the nuclear lamina (a protein network providing nuclear structure) to disruptions in chromatin organization and gene silencing[29].

Resolving centriolar ultrastructure with ExM. The centriole is a cylindrical organelle that is a core component of the centrosome, the main microtubule-organizing centre in animal cells. A mammalian centriole is a ninefold triplet microtubule organized in a circular, radial arrangement, measuring about 400–450 nm long and 200–250 nm wide[131]. Although the overall size of the centriole is above the diffraction limit, the nanoscale spatial arrangement of its constituent proteins, such as the internal cartwheel (a scaffold-like protein assembly at the base that establishes the ninefold symmetry) and the organization of microtubule triplets — three closely associated microtubules (A, B and C tubules) that form the cylindrical wall of a centriole — can

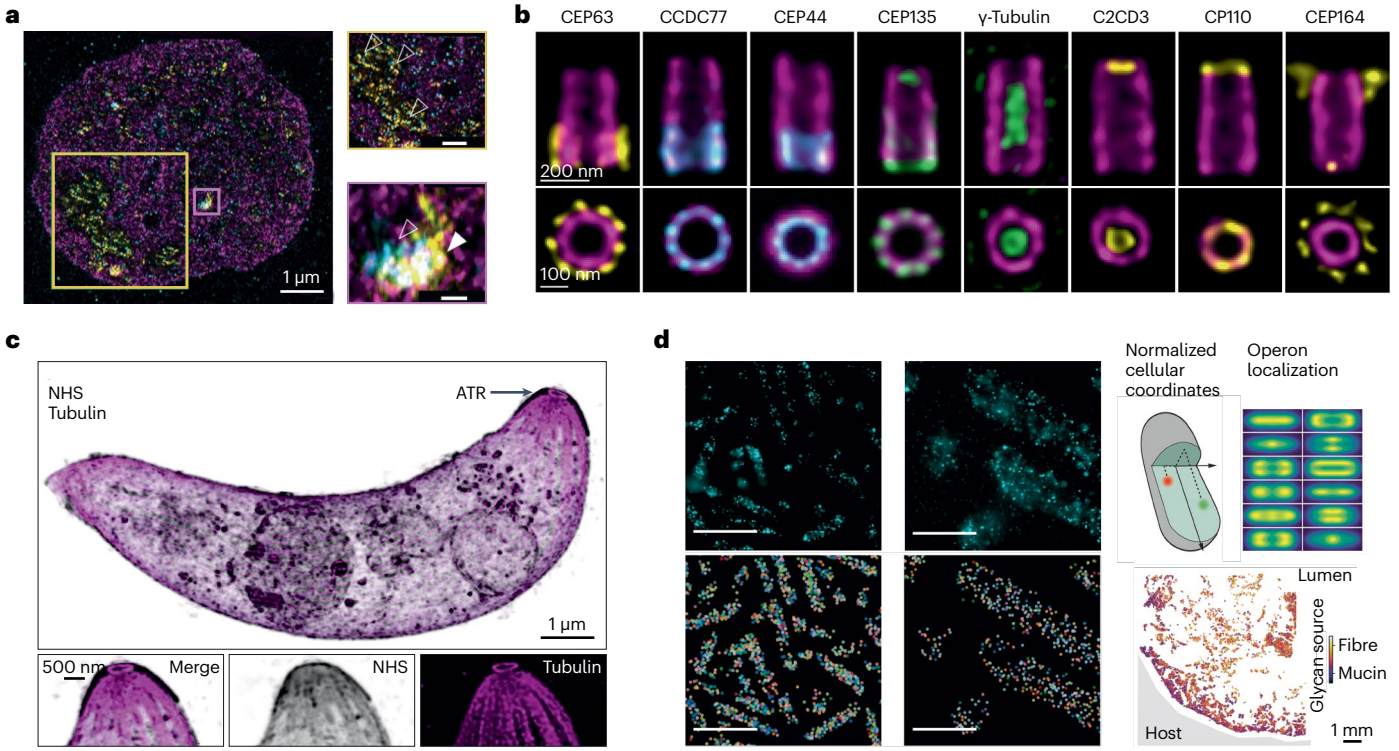

Fig. 3 | Novel biological findings using expansion microscopy. a, Visualizing the machinery of gene expression. Representative image (left) of a nucleus from a zebrafish embryo (a common model organism) obtained using chromatin expansion microscopy. Zebrafish embryos were stained for the transcription factor Nanog (blue), RNA polymerase II (yellow) and DNA (purple). Zoomed-in views (right column) show corresponding yellow and magenta boxed regions from the left image; each shows varied chromatin organization based on enrichment of either Nanog or RNA polymerase II. Arrowheads indicate regions enriched for either Nanog (hollow arrowheads) or RNA polymerase II (solid arrowhead). Scale bar, 1 µm (left), 500 nm (yellow box), 100 nm (magenta box), in biological scale. **b**, Mapping sub-elements of a centriole. Side-view (top row) and top-view (bottom row) images of eight centriolar proteins during the assembly process in human osteosarcoma U2OS cells using ultrastructural expansion microscopy (U-ExM). Each column represents U2OS cells co-stained for tubulin (magenta) with CEP63, CCDC77, CEP44, CEP135, γ-tubulin, C2CD3, CP110 or CEP164. Scale bar, 200 nm (top row) and 100 nm (bottom row), in biological scale. **c**, Revealing the cytoskeleton of parasites. U-ExM image of a *Plasmodium berghei* ookinete immunostained for tubulin (magenta) and stained with *N*-hydroxysuccinimide ester dye (grey). The image of expanded parasite ookinete uncovers the apical tubulin ring (ATR), a conoid-like structure previously thought to be lost in this lineage. Scale bar, 1 µm (top image), 500 nm (bottom row). **d**, Visualizing the transcriptome inside a single bacterium. Images of *Escherichia coli* cells showing individual RNA molecules identified using multiplexed error-robust fluorescence in situ hybridization (MERFISH) in bacteria combined with tenfold robust expansion microscopy. The 50-fold (left column) and 1,000-fold volumetric expansion (right column) allow the physical separation and detection of transcripts. Top and bottom rows represent MERFISH signals and identified transcripts, respectively. Scale bar, 20 µm, in physical scale. NHS, *N*-hydroxysuccinimidyl. Part **a** adapted with permission from ref. 31, AAAS. Part **b** adapted with permission from ref. 132, Elsevier. Part **c** adapted from ref. 144, CC BY 4.0. Part **d** adapted with permission from ref. 90, AAAS.

typically only be resolved by electron microscopy[131]. ExM provides a powerful way to visualize this intricate architecture with molecular specificity. For example, by applying U-ExM to centrioles isolated from *Chlamydomonas* (a single-celled green alga often used as a model organism for studying centrioles), researchers were able to resolve the ninefold symmetry of microtubule cylinders with nanoscale precision comparable to that achieved by direct stochastic optical reconstruction microscopy, a classic super-resolution technique that builds an image by precisely localizing individual fluorescent molecules[21]. When combined with STED, the same study visualized the microtubule triplet structure, a feature typically resolved only by electron microscopy[21]. Beyond static architecture, ExM has been used to map the dynamic process of centriole assembly. Centriole duplication is an essential process that ensures the fidelity of chromosome segregation during cell division. U-ExM was used to map the precise nanoscale distribution of 21 different centriolar proteins (some of which are shown in Fig. 3b) throughout the assembly process. By correlating the spatial location of these proteins with structural features over time, they reconstructed a 4D model (a 3D model that also incorporates the dimension of time) to reveal the chronological sequence of human centriole growth[132].

Nanoscale microbiology with ExM

In the field of microbiology, a central challenge is imaging viruses, microorganisms and their subcellular components, which are often at or below the resolution limit of conventional light microscopy. Detailed structural analysis has been limited to either electron microscopy, which provides nanoscale resolution but struggles with specific biomolecule identification, or standard fluorescence microscopy, which provides molecular identity but lacks sufficient resolution[133–135].

Optical super-resolution techniques such as SMLM and STED have been instrumental in bridging this gap — revealing the nanoscale organization of structures such as the bacterial cytoskeleton[136,137]. However, these methods often require specialized microscopes, specific fluorophores or high laser powers, and achieving high-quality 3D super-resolution deep within complex microbial communities such as biofilms remains a hurdle[137,138]. By physically enlarging these small cells, ExM provides an alternative route to nanoscale imaging that is compatible with standard fluorescent labels and conventional microscopes. Beyond the analysis of single organisms, ExM is also proving to be a valuable tool for studying microorganisms in more complex environments, such as those involved in bacterial biofilms[44,139] and amidst host–pathogen interactions[44,45,140].

Nanoscale imaging of parasites. In parasitology, a key challenge has been to visualize the precise location of specific proteins within organisms. ExM addresses this by providing both nanoscale resolution and molecular specificity through fluorescence labelling, enabling researchers to investigate parasite ultrastructure, developmental stages and key molecules involved with various biological processes[141]. A major application has been in resolving the cytoskeletal structures critical for parasite motility and invasion. For instance, in *Toxoplasma gondii* (a single-celled parasite that can infect some warm-blooded animals), U-ExM was used to map the apical polar ring, a microtubule-organizing centre essential for motility. These studies identified new structural proteins and revealed how they form a multilayered scaffold that is crucial for the ability of the parasite to move and invade host cells[141,142]. Similarly, in the intestinal parasite *Giardia lamblia*, combining ExM with SIM produced highly detailed images of the network of acetylated tubulin[109]. ExM has also provided new insights into the dormant stages of parasites that are critical for chronic infection. *Toxoplasma*, for example, can form a protective, dormant structure called a cyst within host tissue. The dense cyst wall is difficult to study with conventional methods. By using an enhanced U-ExM protocol, researchers were able to visualize the nanoscale organization of proteins within the wall[45]. They discovered that a key secreted protein, previously seen as a smooth signal[143], forms distinct punctate structures distributed throughout the cyst wall matrix. For *Plasmodium* (the parasite that causes malaria), U-ExM was used to show that the *Plasmodium* ookinete retains a vestigial apical tubulin ring, consistent with a reduced conoid-like structure previously thought lost in this lineage[144] (Fig. 3c). Additionally, researchers have used U-ExM to generate a detailed atlas of its development inside red blood cells, cataloging the changing architecture of 13 different organelles and structures across its life cycle[140]. This provides a valuable reference for understanding parasite cell biology, potentially yielding new drug targets.

Resolving bacterial organization from single cells to communities. An *Escherichia coli* cell in its logarithmic growth phase contains thousands of transcripts within a volume of just a few cubic micrometres, a density that makes it difficult to resolve individual RNA molecules with conventional microscopy[90,145]. Although bacterial single-cell RNA sequencing can profile these transcripts, it loses all spatial information. To address this, ExM was combined with multiplexed error-robust FISH (MERFISH) to spatially map transcripts in single bacterial cells[90] (Fig. 3d). This study revealed previously unappreciated intracellular localization patterns for many transcripts. When applied to the gut commensal bacterium *Bacteroides thetaiotaomicron* within mouse colon tissue, the technique showed how these bacteria fine-tune their gene expression depending on their specific location within the colon[90]. ExM has also been used to analyse bacterial biofilms. For example, by expanding a multispecies biofilm, researchers were able to perform proximity analysis at the single-cell level. Their results showed that in a community of three oral bacteria, one species (*Fusobacterium nucleatum*) was in much tighter physical association with a second species (*Streptococcus sanguinis*) than with the third (*Streptococcus mutans*), suggesting stronger adhesive interactions between them and providing insights into how the biofilm is structured[139].

Nanoscale neuroanatomy with ExM

Neuroscience has benefited from ExM because many key neuronal structures, such as the synapses that mediate communication between neurons, are too small to be resolved by diffraction-limited microscopy[9,16,19,71,146]. ExM has helped with the probing of synaptic protein synthesis[33,37], neuronal transcriptome mapping[23,63,147,148], connectomics (comprehensive mapping of how individual neurons are connected to one another)[35,70,75,120,149] and synaptic plasticity[37].

ExM to study local protein synthesis. Although neurotransmission relies on local protein synthesis, whether it occurs in presynaptic terminals of mammalian neurons was difficult to explore using traditional means such as electron microscopy[37,150–155]. ExM was used to demonstrate the presence of ribosomes and mRNAs in axon terminal of neurons of the mouse brain and characterize their distributions in excitatory and inhibitory presynaptic terminals[37]. More recently, tenfold robust expansion was used in combination with STED and SMLM to reveal that axonal endoplasmic reticulum tubules (structures themselves at 20–30 nm in diameter) are frequently in physical contact with ribosomes, often in an activity-dependent manner[33,156].

Mapping brain connectome. A foundational goal in neuroscience is to map the brain's connectome, its comprehensive wiring diagram. This has been challenging owing to the difficulty of tracing densely packed axons and resolving individual synapses[157]. Traditionally, the domain of electron microscopy, ExM, offers a potentially more accessible and higher-throughput approach for mapping brain circuits at single-synapse resolution across various species, including zebrafish, mice, *Drosophila* and *C. elegans*[13,16,35,75,82,83,120,158]. ExM enables high-resolution imaging of brain circuits in large volumes using standard confocal microscopy. For example, the proExM protocol has been successfully applied to brain tissue where individual neurons were colour-coded using Brainbow, a genetic labelling strategy that expresses unique combinations of fluorescent proteins in each neuron[120,159]. The proExM protocol allows for both the preservation of the native fluorescent protein signal and subsequent signal amplification using antibodies that target the fluorescent proteins themselves (anti-FP antibodies). This combined approach made it possible to acquire multicolour, super-resolved images of densely labelled circuits with an effective resolution of ~70 nm after expansion[16]. Another potential advantage is its ability to accelerate the pace of connectomic data acquisition. For instance, by combining ExM with lattice light-sheet microscopy (ExLLSM)[70], researchers were able to complete two-colour, high-resolution imaging of the *Drosophila* central complex in less than 3 days. In a related study using ExLLSM, researchers imaged the *Drosophila* central complex and identified both electrical and chemical presynaptic and postsynaptic sites across a substantial brain volume, a process that would have taken many months with traditional electron

microscopy[36]. A technique called multiround immunostaining EXM (miriEx) has been combined with Brainbow[120]. By integrating miriEx with this dense colour coding, researchers have been able to profile single-neuron morphologies and their connectivity with molecular information, all within the same brain section in a mouse model[120]. More recently, light-microscopy-based connectomics (LICONN)[75] has been reported, via applying an iterative expansion approach with a general 'pan-protein' stain to reconstruct dense brain circuitry. This method combines manual tracing with deep-learning algorithms to yield automated tracing and ultimately a molecularly annotated reconstruction of axons and dendrites throughout a volume[75] (Fig. 4a). Similarly, pan-ExM of tissue (Pan-ExM-t), an adaptation of pan-ExM, also demonstrates its ability to provide rich molecular content of individual synapses and tracing neuronal circuitry, even without applying deep-learning-based segmentation[160].

Visualizing the nanoscale basis of disease

In pathology, ExM allows for the visualization of subtle, disease-related changes in cellular and tissue architecture that are below the resolution limit of conventional light microscopy[14,38,41]. An important factor driving its adoption in biomedical research is its compatibility with clinically relevant FFPE tissue samples, enabling high-resolution studies on archival specimens exhibiting a wide range of diseases[14,38–41,44,45,47,161,162].

Cancer. Many morphological and molecular changes that distinguish cancerous from normal tissue occur at a scale below the diffraction limit of conventional microscopy; such changes have been explored using electron microscopy and super-resolution techniques[163–168]. To date, many types of cancers, such as glioma[39,41], prostate[14], lung[14,42], colon[14], ovary[14], liver[14], colon[14], kidney[14,40,169,170] and metastatic breast cancer[23,162], have been characterized in their morphological and cellular changes via ExM. For example, ExM combined with SRRF revealed disorganized cytoskeletal networks in glioblastoma tumour cells, the most aggressive form of glioma[39,41] (Fig. 4b). ExM was also used to visualize and characterize the interactions between tumour spheroids (serving as in vitro models of solid tumours) and immune cells. For instance, in a renal cell carcinoma tumouroid co-culture system, ExM was used to reveal immune cell infiltration patterns, demonstrating how natural killer (NK92) cells expressing cytosolic GFP navigate and distribute themselves throughout the tumouroid volume[40]. Spatial gene expression analysis of a metastatic breast cancer biopsy sample using ExSeq resolved heterogeneous clusters of tumour cells, immune cells and fibroblast cells within the tumour microenvironment[23]. Owing to its high resolution, ExSeq can identify how gene expression in one cell type changes when it is physically close to another. For instance, ExSeq identified hypoxia-inducible factor-1α (*HIF1A*), a gene commonly associated with metastasis and a predictive marker for therapy resistance[171,172], to be overexpressed in tumour cells only when adjacent to cancer-associated fibroblasts[23,162] (Fig. 4c). ExM has been used to resolve the immunological synapse (~15-nm interface[173]) between activated lymphocytes and target cells[174]. For example, cryo-ExM[56] was used to visualize lytic contents in the synapse between an activated T cell and a chronic myeloid leukaemia cell, including the T cell's granzyme B and perforin-containing granules aimed towards the cancer cell[174].

Neurodegeneration. Alzheimer disease, a common neurodegenerative disease that causes dementia, is associated with the deposition of extracellular amyloid-β (Aβ)-containing plaques, including vascular Aβ deposits, which were poorly resolved by diffraction-limited microscopes[175,176]. ExM combined with SRRF has revealed deposition of microvascular Aβ deposits in the human Alzheimer disease brains[41]. Additionally, other ExM methods have been used to visualize pathophysiological markers in human and mouse brains, showing the distribution and organization of Aβ plaques and α-synuclein aggregates of Alzheimer disease and Parkinson disease, respectively[39,43]. A variant of ExPath, termed dExPath, has been used to assess amyloid plaques in Alzheimer disease[39,177]. dExPath was used to spatially map herpes simplex virus 1 (HSV-1) proteins in Alzheimer disease human brain samples and HSV-1-infected human brain organoids. Although aggregates of hyperphosphorylated tau (p-tau) and Aβ plaques may contribute to the pathogenesis of Alzheimer disease, their fine structure and interactions with other molecules are often beyond the resolution of conventional microscopy. dExPath showed the nanoscale colocalization of p-tau, but not Aβ plaques, with a HSV-1 protein in the entorhinal cortex and hippocampus in human brain samples[39,177] (Fig. 4d).

Infection. ExM enables investigation of bacterial and parasitic infections with nanoscale resolution. One application is tracking how pathogens build themselves using host materials. For example, sphingolipid-ExM was used to investigate whether bacteria incorporate lipids from host cells into their own membranes[46]; infected human cells were supplied with a modified host lipid (a ceramide) that could be fluorescently labelled. Using ExM, they were able to visualize these host lipids being incorporated into both the inner and outer membranes of Gram-negative bacteria such as *Neisseria gonorrhoeae*. This approach provided sufficient resolution to measure the ~30 nm distance between the two bacterial membranes, which previously required electron microscopy[46]. Functional interactions between immune cells and pathogens have also been visualized using ExM. For instance, ExM was used to image an immunological synapse — in this case, the nanoscale interface in which a natural killer immune cell physically contacts a fungal hypha of *Aspergillus fumigatus*[47]. The high-resolution images revealed the polarization and release (or degranulation) of lytic granules, containing toxic proteins such as perforin and granzyme B, from the natural killer cell directly onto the fungus. The study observed that this was associated with visible damage to the mitochondria within the fungus near the synapse, consistent with the killing effect of the immune response[47].

Reproducibility and data deposition

Expected effective resolution and imaging time

In ExM, the final effective spatial resolution is not determined by a single factor but is a function of the physical expansion factor combined with the optical resolution of the microscope used for imaging[9,10]. For example, a standard confocal microscope with a lateral optical resolution of ~300 nm, when used to image a sample expanded by a factor of 4×, will yield an effective lateral resolution of ~75 nm (300 nm/4). If the same microscope is used on a sample expanded 10×, the effective resolution would be 30 nm. Furthermore, if a higher-resolution imaging system, such as a spinning disc confocal with deconvolution that achieves ~150 nm optical resolution, is paired with a 10× expansion protocol, the effective resolution would be ~15 nm (ref. 15). It is important to remember that the practical resolution is also limited by the labelling density, and the linkage error — that is, the size of the label. If the physical distance between the target biomolecule and the fluorophore's anchor point to the hydrogel, is substantial (most common in pre-expansion labelling, but also a possible concern for post-expansion labelling), this would set a limit on localization precision.

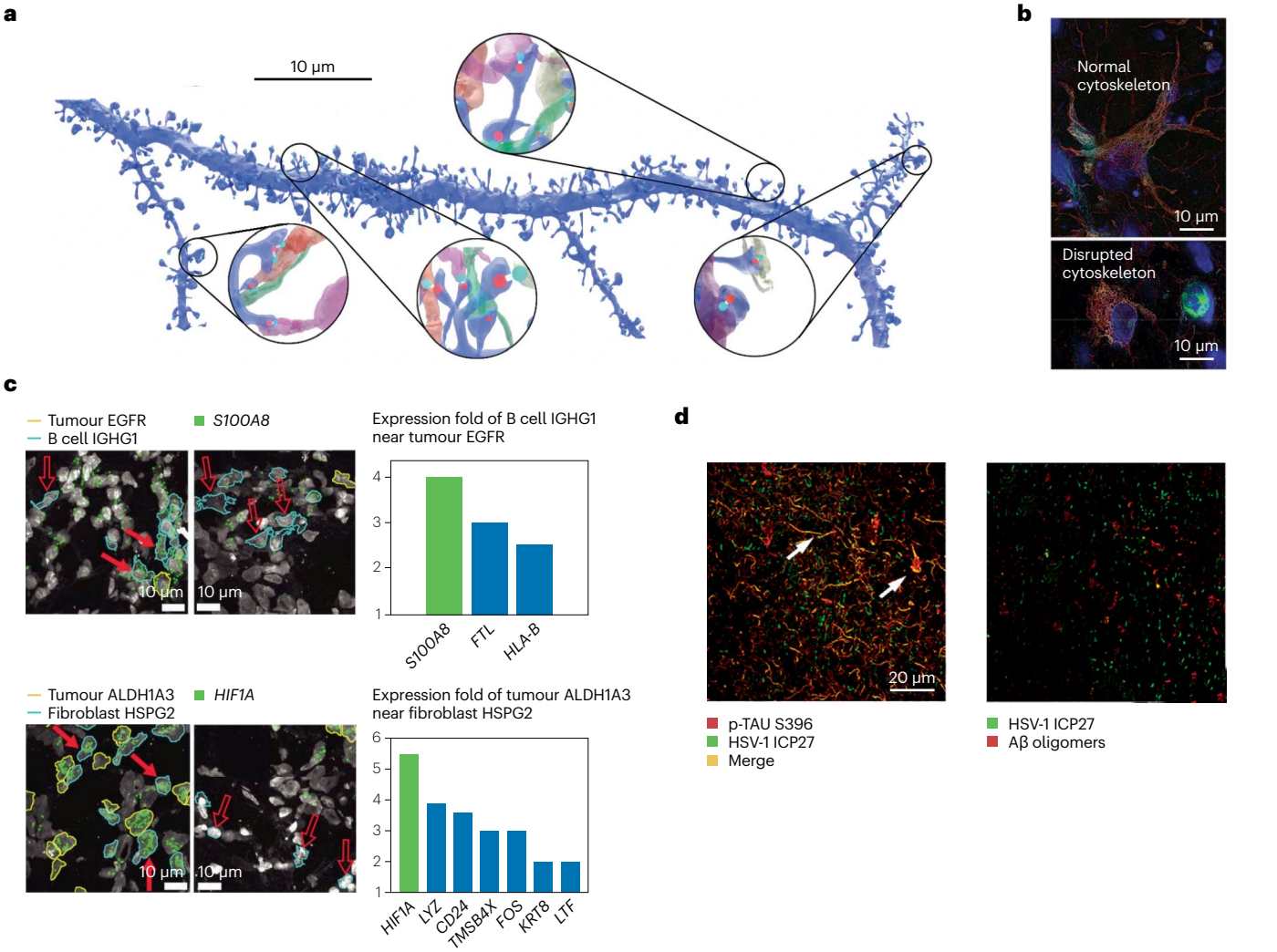

Fig. 4 | Novel biological findings using expansion microscopy. a, Three-dimensional reconstruction of a neural connection. A 3D model of a murine hippocampal neuron's signal-receiving branch (a dendrite) showing its connections (synapses) with other neurons. Murine brains, subject to an iterative expansion microscopy (ExM) approach, were immunostained with presynaptic bassoon (cyan) and postsynaptic SHANK2 (red). The magnified views show synaptically connected boutons. Scale bar, 10 µm, in physical scale. **b**, Comparing healthy versus cancerous cell structures. Images, acquired using ExM combined with super-resolution radial fluctuations, comparing the normal cytoskeleton of a healthy human astrocyte (top) with the disrupted cytoskeleton of an aggressive brain cancer cell (glioblastoma, bottom) in the same sample from a patient with glioblastoma. Cytoskeletal filament network (immunostained for E3 ubiquitin ligase MIB1, green) in the proliferative cancer cell (bottom, immunostained for glial fibrillary acidic protein, orange) is visibly disorganized, compared with the normal cytoskeleton in the non-proliferative healthy astrocyte (top, orange). Scale bar, 10 µm, in biological scale. **c**, Quantifying cell states in cancer. Images of expanded metastatic breast cancer biopsy sample using expansion sequencing showing transcripts of tumour and immune cells. The physical expansion allows for identification and quantification of gene expression changes when different cell types are in close proximity to one another. In the top row, B cells are overexpressed in a biomarker for disease progression, *S100A8*, when adjacent to epidermal growth factor receptor-positive ($EGFR^+$) tumour cells. In the bottom row, $ALDH1A3^+$ tumour cells are overexpressed in the predictive marker for therapy resistance, *HIF1A*, when is in close proximity to cancer-associated fibroblasts. Solid arrows indicate cells in close proximity; hollow arrows indicate cells not in close proximity. Scale bar, 10 µm, in biological scale. **d**, Mapping molecular interactions in neurodegeneration. Images from human brain samples with advanced Alzheimer disease immunostained for herpes simplex virus 1 proteins (HSV-1 ICP27), hyperphosphorylated tau (p-TAU) — a hallmark of Alzheimer disease — and amyloid-β (Aβ) oligomers. Images, acquired using decrowding expansion pathology, show that herpes simplex virus proteins colocalize (white arrows) with p-TAU but not with Aβ oligomers. Scale bar, 20 µm, in physical scale. FTL, ferritin light chain. Part **a** reprinted from ref. 75, Springer Nature Limited. Part **b** reprinted from ref. 41, Springer Nature Limited. Part **c** adapted with permission from ref. 23, AAAS. Part **d** reprinted from ref. 177, CC BY 4.0.

The imaging time in ExM depends on two primary factors: the total (expanded) volume of the sample to be imaged and the acquisition speed of the microscope. This acquisition speed is itself a function of several imaging parameters that differ by microscopy modality. For point-scanning or line-scanning confocal microscopes, the speed is in large part determined by the scanning mechanism

(such as galvanometer scanners) and the resulting scan speed of the laser beam across the sample. This determines the pixel dwell time — the detector integration per pixel — and together with the total pixel count, sets the overall frame time. For camera-based systems such as spinning disc, wide-field or light-sheet microscopy, the speed is determined in large part by the camera exposure time for each captured image. In all cases, these timing parameters are also governed by the illumination intensity (laser or light-emitting diode power); higher illumination may permit shorter dwell or exposure times, for a given SNR, but in turn may increase the risk of photobleaching[178].

Because the sample volume increases by the cube of the linear expansion factor (for example, a 4× linear expansion results in a 64× increase in volume), acquiring images throughout an entire expanded sample with a high magnification lens is more time-consuming than for the unexpanded sample. For instance, imaging a 25 µm × 25 µm biological region with 100 nm pixels requires a 250 × 250 pixel image. After 4× expansion, this region becomes 100 µm × 100 µm. To properly sample newly revealed, higher-resolution details, one might use the same 100 nm microscope pixel size, which now corresponds to a 25 nm effective biological pixel size. This would require acquiring a 1,000 × 1,000 pixel image — a 16-fold increase in pixel number for the same biological area — directly increasing the imaging time. Moreover, fluorophores will have also been diluted by 64×, producing dimmer images and potentially necessitating longer exposures or higher illumination. This trade-off can be mitigated by using inherently fast imaging systems, such as spinning disc or light-sheet microscopes, the latter of which can be particularly well suited for large-volume imaging. A practical strategy is often to first acquire a low-magnification overview scan of the expanded sample to identify regions of interest, which can then be targeted for slower, higher-resolution imaging, thus optimizing the use of microscope time[146].

Reporting standards and data deposition

To promote transparency and reproducibility in the community, adhering to reporting standards when publishing ExM data is essential. For an experiment to be reproducible, key methodological details must be documented. This includes all aspects of sample preparation, such as fixation conditions, anchoring chemistry, gel composition and the specific softening method chemistry used. The measured expansion factor and the method used to determine it (for example, measurement of tissue size before versus after expansion) should be clearly stated. Distortion analysis is required when introducing a new ExM protocol or applying an existing one to a previously unreported specimen type. Pre-expansion and post-expansion imaging of the same region remains the most common validation approach, often using aligned images to quantify distortion, for example, <1–4% over typical fields of view[9,19] (Fig. 5a,b). Internal ultrastructural references, such as cilia[15,20,179], microtubules[12,61,94] or nuclear pore complexes[19,20,94,180], may also be used (Fig. 5c–e). Alternative methods such as GelMAP[181] have emerged (Fig. 5f), using microfabricated fluorescent grids imprinted into gels to enable local expansion-factor measurement, deformation field mapping[9,16] and nonlinear correction (via BigWarp). GelMap[181] offers precise, field-of-view-wide analysis and has been applied in some studies (for example, U-ExM in HIV-1 imaging[182]). Although GelMAP provides a powerful benchmark where available but requires specialized plates and computational pipelines, pre/post-comparison and internal ruler methods are more commonly used for routine validation of new ExM methods. Reporting must also detail the labelling and imaging strategy, including whether staining was pre-expansion or post-expansion, the specific probes used and all relevant imaging parameters such as microscope type, objective magnification and NA, pixel size, laser powers, exposure times and *Z*-stack intervals if appropriate[52,146]. Furthermore, any computational data processing steps, such as the algorithms used for deconvolution, stitching or background subtraction, should be clearly described. To complete this commitment to transparency and enable re-analysis by others, raw and processed image data should be deposited in a public data repository that follows FAIR (Findable, Accessible, Interoperable and Reusable) data-sharing principles[183].

Limitations and optimizations

ExM has democratized nanoscale imaging by enabling super-resolution visualization with conventional microscopes. However, similar to any other tool, it has limitations that researchers should consider. This section outlines these challenges and highlights potential solutions and optimizations.

Requirement for fixed samples

A primary constraint of all ExM protocols is their incompatibility with live-cell imaging. The chemical and physical processes involved in hydrogel embedding, softening and expansion inevitably disrupt native molecular interactions and thus cellular viability, precluding the study of dynamic biological processes over time. Although direct live-cell ExM is not feasible, researchers can perform imaging of live samples for a precise duration immediately before rapid fixation and subsequent ExM processing, to gain temporal context[16,119,181], although this does not capture any dynamics during or after expansion.

Signal dilution and amplification

The physical expansion of samples reduces the concentration of fluorophores, leading to signal dilution[184]. This can sometimes be compensated for by increasing illumination intensity or detector gain, but these adjustments must be balanced against photobleaching and reduced imaging speed. When imaging low-abundance targets or using very high expansion factors, high-NA objectives can help but, in some cases, dedicated signal amplification strategies are required. These include enzymatic methods such as tyramide signal amplification, which uses horseradish peroxidase to covalently deposit a high density of fluorophores[122]. More recently, highly multiplexable, enzyme-free DNA-based methods have been widely adopted. These strategies use anchored targets (such as RNA in ExFISH[24] or DNA-barcoded antibodies[185]) to initiate in-gel amplification, such as HCR[186,187], biotin–streptavidin-based amplification systems[106,107,122] or rolling circle amplification as used in ExSeq[23]. Alternatively, methods such as Immuno-SABER use pre-formed DNA concatemers to build a bright, programmable signal, providing a high-gain, multiplex-friendly solution to overcome signal dilution[24,114,122,188,189].

Expansion heterogeneity and deformations

A critical limitation for quantitative work is expansion heterogeneity, in which expansion factors vary locally, introducing anisotropy and distortions. Typically, root mean square errors of 1–2% over a field of view (~10–50 µm) are reported[9,16]. For nanoscale measurements, it is crucial to understand what this means: a 1–2% error translates to an ~1–2 nm distortion per 100 nm distance. This may be tolerable for most qualitative studies but is a key consideration for precise measurements, such as the diameter of an ~40 nm synaptic vesicle or the width of an ~20–30 nm synapse cleft. Sources of this variation are

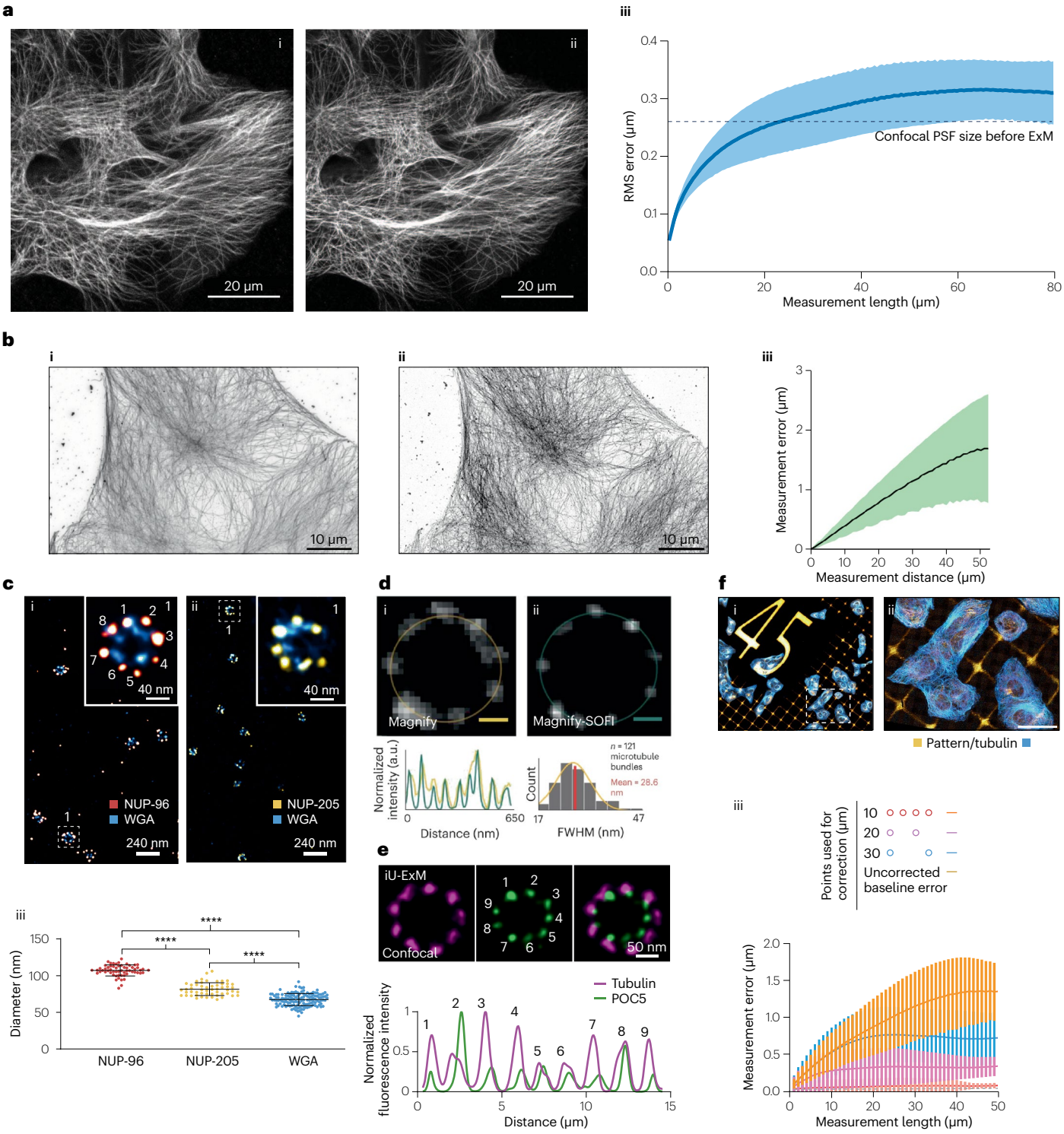

both procedural and sample-intrinsic. They can include pipetting inconsistencies in monomer solutions, incomplete or uneven softening (especially in dense, ECM-rich or unevenly fixed tissues), sample density differences and mounting effects such as gel compression. This highlights a critical point for new practitioners: applying a protocol to a new sample type not covered in the original publication will sometimes require re-optimization, as parameters such as the duration, temperature or chemical composition of the digestion or denaturation steps may need to be adjusted. It should always be remembered that any image of a once-living specimen is an imperfect representation. ExM adds further steps of gelation, digestion and expansion that can perturb ultrastructure, so careful case-by-case validation is

Fig. 5 | Assessment of expansion quality for a new expansion protocol. New expansion microscopy (ExM) protocols are validated to ensure that the expansion is uniform (isotropic) and the expansion factor is consistent. Common validation methods include direct distortion measurement and the use of biological structures with known dimensions as internal nanoscale rulers. **a**,**b**, Direct distortion measurement. Pre-expansion and post-expansion images of the same structure are compared to quantify distortion. **a**, Images of the human cell line HEK293 immunostained for microtubules (grey) are shown before (part **ai**) and after (part **aii**) 4.5× expansion. The graph (part **aiii**) plots the measurement error between the images in parts **ai** and **aii**, confirming low distortion (<1% of the measured distance). The blue line and blue shaded area represent the mean error values and standard deviation. Scale bar, 20 µm, in biological scale. **b**, A similar comparison between a super-resolution stimulated emission depletion microscope for the pre-expansion image (part **bi**) of the monkey fibroblast cell line COS7 immunostained for microtubules (grey) and a confocal microscope for the 10× expanded image in part **bii** of the same cell. The graph (part **biii**) plots the measurement error between images in parts **bi** and **bii**. The black line and green shaded area represent the mean error values and standard deviation. Scale bar, 10 µm, in biological scale. **c**–**e**, Using internal biological structures as nanoscale rulers to evaluate expansion factor and quality. **c**, Images of the nuclear pore complex (NPC), which has a stable diameter. Immunostaining for outer ring component NUP-96 (part **ci**) or inner ring component NUP-205 (part **cii**), with wheat germ agglutinin (WGA) marking the central channel and the insets show magnified view of the dashed boxes. The plot (part **ciii**) shows measured diameters of the NPC rings labelled by various markers. Scale bar, 240 nm (part **ci**) and (part **cii**); insets: 40 nm, in biological scale. **d**, Images of human airway cilia. **di**, Cross-section of basal bodies from a human lung organoid stained with *N*-hydroxysuccinimide ester (grey) imaged with Magnify revealing their internal ninefold microtubule symmetry. **dii**, Imaged with Magnify combined with super-resolution optical fluctuation (Magnify-SOFI), with plots quantifying the size and spacing of internal microtubule components. Scale bar, 50 nm in biological scale, (part **di**) and (part **dii**). **e**, Image of mouse photoreceptor connecting cilium. Ninefold organization of microtubule double-stained for tubulin and POC5 revealed using iterative ultrastructure ExM (iU-ExM), with plots profiling their signals. Scale bar, 50 nm. **f**, Using expandable and scalable rulers to determine expansion factors. Embedding microfabricated fluorescent reference grids into gels to enable precise local expansion-factor measurement. U2OS cells imaged before expansion (part **fi**) and after expansion (part **fii**) (expansion factor, 9.6×) using tenfold robust expansion microscopy, corrected using GelMap. Stained tubulin (cyan) in cells cultured directly on laminin-patterned coverslip (laminin is an extracellular matrix protein and conjugated with fluorophore (orange)). An example of the measurement of deformation and the schematic of landmark spacing used for pattern correction (part **fiii**). This method highlights the importance of local quality control in contributing to standardized quantitative measurements in the ExM. The dashed line indicates baseline error owing to manual landmark selection (rescaling the pre-expansion tubulin channel to the post-expansion dimensions and then registering it to the original image). Scale bar, 400 µm (part **fi**) and 40 µm (part **fii**) in biological scale. ****$P < 0.0001$. a.u., arbitrary unit; FWHM, full-width half maximum; PSF, point-spread function; RMS, root mean square. Part **a** reprinted with permission from ref. 9, AAAS. Part **b** adapted from ref. 19, CC BY 4.0. Parts **c** and **e** adapted from ref. 179, CC BY 4.0. Part **d** adapted from ref. 15, Springer Nature Limited. Part **f** adapted from ref. 181, Springer Nature Limited.

essential. Various methods exist to calibrate these distortions, from using internal biological rulers to more advanced, grid-based mapping techniques.

Outlook

Advancing biomolecule retention

An ongoing pursuit in the ExM field is the development of more universal and efficient anchoring strategies. Although methods such as Magnify have broadened the scope of retainable biomolecules[15,28,44], future research may yield novel hydrogel chemistries or multifunctional linkers to capture an even wider array of biological targets. For example, new chemistries could be developed to covalently bind molecules via functional groups other than the commonly targeted primary amines, such as targeting carboxyl groups on acidic amino acids or hydroxyl groups on sugars and post-translationally modified proteins. The ideal would be strategies that are less sensitive to tissue type or fixation history, ensuring more uniform and complete biomolecule retention across diverse experimental contexts. A particularly challenging frontier within this area is the efficient anchoring and visualization of small metabolites, ions and other objects with few-to-no easily anchorable motifs. Current ExM protocols are primarily optimized for larger macromolecules such as proteins, nucleic acids and lipids. However, the ability to map the precise nanoscale distribution of small metabolites in situ — such as sugars or specific neurotransmitters — would provide profound insights into cellular function, signalling and disease states. Achieving this will require significant innovation in rapid, in situ chemical fixation and anchoring strategies that can capture these highly diffusible molecules before they are lost during processing.

Towards ultimate resolution

Another frontier in the ExM field is the push towards its ultimate resolution, with the goal of visualizing the shapes of individual proteins and their complexes or even smaller molecules. The ultimate resolution of ExM is unknown: although the mesh size, or spacing between polymer threads, is 1–2 nm (refs. 190,191), and the inhomogeneity size is thought to be 10–20 nm (refs. 192,193), it is possible that the expansion error itself could be smaller, as each node in the network is being pulled on by multiple polymer threads, resulting in some 'cancelling out' of error. This is a hypothesis that needs to be tested further. The hydrogel's mesh size and chemical composition are critical, interdependent parameters. The final expansion factor is not determined by monomer density alone, but by a balance between the outward osmotic pressure driving swelling and the network's elastic resistance. Protocols achieve different expansion factors by precisely tuning this balance, often by varying the ratio of charged polyelectrolyte monomers (such as SA) to neutral monomers (such as AA). A higher ratio of charged monomers increases the internal osmotic pressure, driving a larger expansion.

Mesh size also fundamentally impacts the labelling strategy. Recent single-molecule measurements using hydrogels with tunable expansion have precisely quantified this effect[194], showing that diffusion is strikingly size-dependent. For example, in a dense, partially expanded gel (1.66× expansion), the diffusion of a 150 kDa IgG antibody was suppressed by ~50%. By contrast, in a highly expanded gel (3.31× expansion), the same IgG diffused almost as freely as it would in a solution without a gel matrix. This finding provides a clear physical mechanism for post-expansion labelling: the 4x expansion opens the gel mesh sufficiently to allow for the free diffusion of probes such as antibodies that would be severely hindered or blocked in the unexpanded state.

Imaging ExM-expanded samples on existing super-resolution microscopes has yielded images with higher resolution than achievable by either technology alone. A growing body of work has explored this synergy (Table 2). For example, the one-step nanoscale expansion[74] protocol combined 10× expansion with SRRF to report sub-1 nm effective

Glossary

Anchoring
The process of covalently linking biomolecules or labels to the hydrogel network, thereby retaining their spatial fidelity during tissue expansion.

Anchoring agents
A chemical linker (Acryloyl-X) that forms a covalent bond between biomolecules of interest and the hydrogel network, ensuring that they are retained and move apart with the gel during expansion.

Decrowding
The physical separation of biomolecules from one another by isotropic hydrogel expansion, which reduces molecular crowding and steric hindrance to improve epitope accessibility and imaging resolution.

Diffraction limit
The fundamental resolution limit in classical light microscopy, typically around 200–300 nm, defined as the smallest resolvable distance between two objects. Expansion microscopy is designed to overcome this limit.

Distortion
Any deviation from perfectly isotropic expansion, which would result in the deformation of structures and an inaccurate representation of their true biological shape and organization.

Expansion factors
The linear fold increase in size of a sample after expansion. For example, a 4× expansion factor means a structure becomes four times longer in each dimension.

Hydrogel
A 3D network of polymer chains that can absorb large amounts of water and swell. In expansion microscopy, hydrogels are synthesized in situ from a solution of monomers (acrylamide) and crosslinkers (*N*,*N*′-methylenebisacrylamide) that polymerize around a sample's biomolecules.

Isotropy
In the context of expansion microscopy, the property of expanding uniformly in all three spatial directions. Isotropic expansion is essential for accurately preserving the original shape and relative spatial relationships of molecules and cellular structures in the magnified sample.

Softening
The process of enzymatically or chemically breaking down the native structural components of a biological sample after it is embedded in the hydrogel. Molecules are either separated, or fragmented, depending on the scientific goal. This softening of mechanical rigidity is crucial for allowing the sample to expand uniformly with the gel.

resolution, allowing for the visualization of individual protein shapes (the proteins were anchored to the hydrogel, chopped into pieces with proteinase K and then the fragments pulled apart and nonspecifically stained). Beyond fluorescence, ExM has also been paired with label-free methods such as vibrational imaging (for example, MAGNIFIERS[195] and VISTA[196,197]) to achieve high-resolution chemical imaging (Table 2). Other approaches aim to engineer more uniform and defect-free hydrogel networks. For example, changing the monomer structure to tetrahedral and the assembly method away from free radical polymerization, as in Tetra-gel[198], can create a more uniform diamond lattice with ~1 nm mesh, reducing expansion error and distortion to low single digits. Although these cutting-edge methods demonstrate the exciting potential of ExM, they are still emerging and may require further validation by the broader scientific community to confirm their robustness and general applicability.

Towards standardized, automated and scalable ExM workflows

Exploring standardization, automation and scalability could enable larger-scale biological inquiries with highly consistent results[146]. This trend includes an increasing emphasis on well-characterized and quality-controlled reagents, with some protocols already being offered as comprehensive kits[15,181,199] that provide validated materials and standardized instructions for specific sample types. To further enhance consistency and enable high-throughput studies for large-scale experiments and potential clinical applications[14], automation[200,201] may be a key future direction[146,201]. This includes the development of robotic and microfluidics-based systems designed to streamline multistep processes such as sample handling, hydrogel embedding and multiround staining. Envisioned are fully automated, 'turn-key' ExM sample processing platforms that could integrate multiple steps, from initial sample preparation through staining and perhaps even direct transfer to imaging systems, analogous to current high-throughput platforms in genomics or automated histology. Furthermore, integrating machine learning into these automated workflows could optimize imaging parameters in real-time and streamline data analysis, enhancing experimental efficiency and potentially helping support future development of ExM-based diagnostic applications.

Integrating spatial omics with ExM

ExM is facilitating a range of spatial omics technologies (Table 2). This convergence is anticipated to allow researchers to overlay enhanced structural details offered by tissue expansion with more comprehensive molecular data. ExM decrowds RNA molecules, which enables more precise interrogation of RNA identity, especially when the same punctum must be followed over many cycles of staining, imaging and washing[23–25,27,63,64,147,188]. Traditional single-cell RNA sequencing provides transcriptomic profiles but lacks spatial resolution to map RNAs within cells, whereas conventional FISH cannot resolve many different transcripts in the same sample. Variants of ExM that increase distances between RNA molecules have been applied to a range of tissue types, from cell culture to thin tissue sections to whole organs[23,24,147,188]. ExFISH enabled multiplexed RNA detection in cell culture and tissue[24]. In the mouse brain, Ex-ST[27] enabled detection of more cell-type-specific transcripts (>80%) than Visium alone (50%). Methods such as ExSeq[23] and expansion-compatible MERFISH[25] can be used to map numerous RNA species within expanded cellular or tissue context, with higher yield than their unexpanded counterparts. ExSeq[23], for example, enables targeted or untargeted in situ sequencing of RNA transcripts directly within a hydrogel-expanded sample. ExSeq was used to map 42 genes related to key excitatory and inhibitory cell types, highlighting their layer-specific spatial distribution in mouse primary visual cortex[23]. At a finer, subcellular level, ExSeq has also been used to visualize RNAs inside neuronal dendrites and spines[23]. Similarly, by applying the EASI-FISH method to thick brain sections, researchers have created multiplexed maps of gene expression that revealed previously unknown spatially organized subregions in the lateral hypothalamus[63]. MERFISH[25] uses a combinatorial strategy in which each RNA species is assigned a unique binary barcode. Through sequential rounds of hybridization and imaging, this barcode is read out, allowing for the identification of hundreds to thousands of different RNA species. Physical expansion helps to separate RNA signals that might otherwise overlap, making it easier to distinguish and decode individual transcripts, especially for highly expressed or densely packed RNAs. ExM allows for more accurate assignment of decoded RNA signals to specific cells and their ultrastructurally

defined subcellular compartments[23–25,27,63]. Future work in this area may focus on increasing multiplexing capacity and enhancing the speed of these workflows.

Complementing RNA-focused methods, recent innovations in iterative staining and barcoding have expanded the utility of ExM for high-plex protein imaging, enabling multianalyte spatial omics. For instance, iterative indirect immunofluorescence combined with ExM allows sequential staining of 10+ protein targets in the same sample, revealing nanoscopic nuclear lamina networks at ~50 nm resolution[53]. Similarly, DNA-barcoded antibodies coupled with HCR can be applied to expanded tissues to facilitate multiplexed detection of up to 30 proteins, improving signal amplification and reducing crosstalk[185]. These approaches, when integrated with RNA omics (for example, ExSeq[23]), promise comprehensive multianalyte mapping with subcellular resolution.

In the realm of proteomics and beyond, ExM combined with techniques for molecular identification is an emerging direction for broader, discovery-based spatial proteomics and lipidomics, especially untargeted methods enhanced by ExM's resolution boost (Table 2). Although highly multiplexed immunofluorescence on expanded samples provides structural information, integration with mass spectrometry (MS) imaging is an emerging direction for broader, discovery-based spatial proteomics and lipidomics (Table 2). By applying MS imaging techniques to expanded tissues — such as those described for ExM-based liquid chromatography–MS (ExM-LC–MS/MS)[202], ProteomEx[203], tissue-expansion MS[204] or gel-assisted mass spectrometry imaging[205] and ExPRESSO[206], which creates vacuum-stable gels for high-plex (>40 markers) analysis on platforms such as multiplexed ion beam imaging and imaging mass cytometry — researchers aim to map the distribution of specific endogenous proteins, peptides or lipids at high spatial resolution. In situ imaging proteomics via expansion (iPEX) integrates isotropic tissue expansion with matrix-assisted laser desorption/ionization mass spectrometry imaging to enable untargeted, micrometre-resolution (1–5 µm effective pixel size) deep proteomics in diverse samples such as mouse retina, brain (including Alzheimer models), intestine, liver, cerebellum and human cerebral organoids[207]. iPEX achieves 10–100-fold sensitivity gains, identifying 600–1,500 proteins with high-precision spatial maps, revealing layer-specific peptides and early disease markers (for example, mitochondrial aberrancy in Alzheimer disease). This points to future efforts in scaling untargeted omics for whole-organ mapping, increasing sensitivity for low-abundance molecules and easing integration with correlative workflows for multi-omic insights into cellular heterogeneity and disease mechanisms.

Expanding ExM's reach: from complex tissues to large-scale systems

A key trajectory for expanding the impact of ExM involves enhancing its applicability to a broader diversity of biological systems. This includes both specimens that are inherently challenging owing to their material properties and those that are physically large, such as intact organs or even organisms, which present distinct but often overlapping hurdles for sample processing and effective imaging. Specialized softening strategies have enabled the application of ExM to a range of challenging specimens, from tissues rich in ECM to organisms with tough cell walls, and ongoing work continues to push these boundaries. For example, protocols such as Mosquito Tissue Ultrastructure-Expansion Microscopy (MoTissU-ExM)[208] have been developed to handle the tough, chitinous cuticle of mosquito disease vectors, enabling ultrastructural analysis of parasites such as *Plasmodium* within host tissues. In a remarkable demonstration of this adaptability, U-ExM was recently applied to more than 200 species of cultured planktonic eukaryotes — organisms that are often small, difficult to culture and resistant to standard labelling — to assign molecular identities to ultrastructures previously only visible by electron microscopy, opening a new path for environmental cell biology[209].

Concurrently, ExM protocols are being refined for physically large-scale specimens. For example, methods for whole *C. elegans* (ExCel)[82] and zebrafish embryos[83] must be optimized for both tough cuticles and large volumes. Other protocols are designed for even larger specimens, for example, whole mouse brains, intact kidneys, other organs or even organisms, which can be many millimetres to centimetres in scale before expansion[55,66]. Ensuring uniform anchoring and gelation, complete softening, uniform expansion and deep, consistent labelling throughout extensive volumes is a hurdle that may require further protocol optimization in certain contexts. Subsequently, imaging these physically massive, expanded hydrogels is pushing the limits of current microscopy systems in terms of field of view, objective working distance, data acquisition speed and management of the ensuing large datasets. Light-sheet systems such as expansion-assisted selective plane illumination microscopy[210] have been used for capturing images throughout large, expanded samples, such as entire mouse brain[211], and there are opportunities for innovations in microscope design and optical systems specifically engineered for unique, multi-centimetre-scale, transparent hydrogels. This includes the potential development of objectives with exceptionally LWDs and very large fields of view, while maintaining sufficient NA for high-resolution imaging. Collectively, these parallel advancements in both tailored ExM protocols for diverse and large specimens, alongside dedicated imaging technologies, will allow high-resolution 3D whole-organ biomolecule mapping, expanding ExM's utility in fields such as developmental biology, neuroscience and pathology.

Published online: 16 April 2026

References

1. Lelek, M. et al. Single-molecule localization microscopy. *Nat. Rev. Methods Primers* **1**, 39 (2021).
2. Lukinavičius, G. et al. Stimulated emission depletion microscopy. *Nat. Rev. Methods Primers* **4**, 56 (2024).
3. Vicidomini, G., Bianchini, P. & Diaspro, A. STED super-resolved microscopy. *Nat. Methods* **15**, 173–182 (2018).
4. Balzarotti, F. et al. Nanometer resolution imaging and tracking of fluorescent molecules with minimal photon fluxes. *Science* **355**, 606–612 (2017).
5. Eilers, Y., Ta, H., Gwosch, K. C., Balzarotti, F. & Hell, S. W. MINFLUX monitors rapid molecular jumps with superior spatiotemporal resolution. *Proc. Natl Acad. Sci. USA* **115**, 6117–6122 (2018).
6. Gwosch, K. C. et al. MINFLUX nanoscopy delivers 3D multicolor nanometer resolution in cells. *Nat. Methods* **17**, 217–224 (2020).
7. Moosmayer, T. et al. MINFLUX fluorescence nanoscopy in biological tissue. *Proc. Natl Acad. Sci. USA* **121**, e2422020121 (2024).
8. Schmidt, R. et al. MINFLUX nanometer-scale 3D imaging and microsecond-range tracking on a common fluorescence microscope. *Nat. Commun.* **12**, 1478 (2021).
9. Chen, F., Tillberg, P. W. & Boyden, E. S. Expansion microscopy. *Science* **347**, 543–548 (2015).
   This paper introduced the paradigm of expansion microscopy, a method that achieves nanoscale resolution by physically magnifying biological specimens permeated by a swellable hydrogel, thereby opening up super-resolution capability to laboratories with conventional microscopes.
10. Truckenbrodt, S. et al. ×10 expansion microscopy enables 25-nm resolution on conventional microscopes. *EMBO Rep.* **19**, e45836 (2018).
    The authors introduce an expansion microscopy protocol that achieves ~25-nm resolution through improvements in the hydrogel chemistry.
11. Wang, S. et al. Single-shot 20-fold expansion microscopy. *Nat. Methods* **21**, 2128–2134 (2024).

12. Chang, J.-B. et al. Iterative expansion microscopy. *Nat. Methods* **14**, 593–599 (2017).
13. Sim, J. et al. Nanoscale resolution imaging of whole mouse embryos using expansion microscopy. *ACS Nano* **19**, 7910–7927 (2025).
14. Zhao, Y. et al. Nanoscale imaging of clinical specimens using pathology-optimized expansion microscopy. *Nat. Biotechnol.* **35**, 757–764 (2017).
This work describes an expansion microscopy protocol optimized for pathology, enabling the nanoscale imaging of clinically relevant FFPE tissue specimens using conventional microscopes.
15. Klimas, A. et al. Magnify is a universal molecular anchoring strategy for expansion microscopy. *Nat. Biotechnol.* **41**, 858–869 (2023).
This work introduces an ExM variant that uses a broad-spectrum and concurrent anchoring strategy to retain proteins, nucleic acids and lipids.
16. Tillberg, P. W. et al. Protein-retention expansion microscopy of cells and tissues labeled using standard fluorescent proteins and antibodies. *Nat. Biotechnol.* **34**, 987–992 (2016).
This work describes a widely adopted ExM method that enables robust nanoscale imaging of proteins by demonstrating compatibility with standard, commercially available antibodies and genetically encoded fluorescent proteins.
17. Chozinski, T. J. et al. Expansion microscopy with conventional antibodies and fluorescent proteins. *Nat. Methods* **13**, 485–488 (2016).
18. Faulkner, E. L. et al. Imaging nanoscale nuclear structures with expansion microscopy. *J. Cell Sci.* **135**, jcs259009 (2022).
19. Damstra, H. G. et al. Visualizing cellular and tissue ultrastructure using ten-fold robust expansion microscopy (TREx). *eLife* **11**, e73775 (2022).
20. Pesce, L., Cozzolino, M., Lanzanò, L., Diaspro, A. & Bianchini, P. Measuring expansion from macro- to nanoscale using NPC as intrinsic reporter. *J. Biophoton.* **12**, e201900018 (2019).
21. Gambarotto, D. et al. Imaging cellular ultrastructures using expansion microscopy (U-ExM). *Nat. Methods* **16**, 71–74 (2019).
22. Dolgin, E. 'Expansion microscopy' turns ten: how a tissue-swelling method brought super-resolution imaging to the masses. *Nature* **637**, 752–754 (2025).
23. Alon, S. et al. Expansion sequencing: spatially precise in situ transcriptomics in intact biological systems. *Science* **371**, eaax2656 (2021).
This work presents a method that integrates ExM with in situ RNA sequencing to enable transcriptomic mapping with nanoscale spatial precision within intact biological systems.
24. Chen, F. et al. Nanoscale imaging of RNA with expansion microscopy. *Nat. Methods* **13**, 679–684 (2016).
This work reports an ExM method for RNA imaging by developing a chemical strategy to anchor transcripts to the hydrogel, enabling nanoscale spatial mapping of individual RNA molecules in cells and tissues.
25. Wang, G., Moffitt, J. R. & Zhuang, X. Multiplexed imaging of high-density libraries of RNAs with MERFISH and expansion microscopy. *Sci. Rep.* **8**, 4847 (2018).
26. Acke, A. et al. Expansion microscopy allows high resolution single cell analysis of epigenetic readers. *Nucleic Acids Res.* **50**, e100 (2022).
27. Fan, Y. et al. Expansion spatial transcriptomics. *Nat. Methods* **20**, 1179–1182 (2023).
28. Cui, Y. et al. Expansion microscopy using a single anchor molecule for high-yield multiplexed imaging of proteins and RNAs. *PLoS ONE* **18**, e0291506 (2023).
29. Payne, A. C. et al. In situ genome sequencing resolves DNA sequence and structure in intact biological samples. *Science* **371**, eaay3446 (2021).
30. Woodworth, M. A. et al. Multiplexed single-cell profiling of chromatin states at genomic loci by expansion microscopy. *Nucleic Acids Res.* **49**, e82 (2021).
31. Pownall, M. E. et al. Chromatin expansion microscopy reveals nanoscale organization of transcription and chromatin. *Science* **381**, 92–100 (2023).
32. Gallagher, B. R. & Zhao, Y. Expansion microscopy: a powerful nanoscale imaging tool for neuroscientists. *Neurobiol. Dis.* **154**, 105362 (2021).
33. Koppers, M. et al. Axonal endoplasmic reticulum tubules control local translation via P180/RRBP1-mediated ribosome interactions. *Dev. Cell* **59**, 2053–2068.e9 (2024).
34. Jiang, N. et al. Superresolution imaging of *Drosophila* tissues using expansion microscopy. *Mol. Biol. Cell* **29**, 1413–1421 (2018).
35. Behzadi, S. et al. Expansion microscopy reveals neural circuit organization in genetic animal models. *Neurophotonics* **12**, 010601 (2025).
36. Lillvis, J. L. et al. Rapid reconstruction of neural circuits using tissue expansion and light sheet microscopy. *eLife* **11**, e81248 (2022).
37. Hafner, A.-S., Donlin-Asp, P. G., Leitch, B., Herzog, E. & Schuman, E. M. Local protein synthesis is a ubiquitous feature of neuronal pre- and postsynaptic compartments. *Science* **364**, eaau3644 (2019).
38. Bucur, O. et al. Nanoscale imaging of clinical specimens using conventional and rapid-expansion pathology. *Nat. Protoc.* **15**, 1649–1672 (2020).
39. Valdes, P. A. et al. Improved immunostaining of nanostructures and cells in human brain specimens through expansion-mediated protein decrowding. *Sci. Transl. Med.* **16**, eabo0049 (2024).
40. Edwards, S. J. et al. High-resolution imaging of tumor spheroids and organoids enabled by expansion microscopy. *Front. Mol. Biosci.* **7**, 208 (2020).
41. Kylies, D. et al. Expansion-enhanced super-resolution radial fluctuations enable nanoscale molecular profiling of pathology specimens. *Nat. Nanotechnol.* **18**, 336–342 (2023).
42. Application of ethyl cinnamate based optical tissue clearing and expansion microscopy combined with retrograde perfusion for 3D lung imaging. *Exp. Lung Res.* **46**, 393–408 (2020).
43. Kang, J. et al. Multiplexed expansion revealing for imaging multiprotein nanostructures in healthy and diseased brain. *Nat. Commun.* **15**, 9722 (2024).
44. Cheng, Z. et al. MicroMagnify: a multiplexed expansion microscopy method for pathogens and infected tissues. *Adv. Sci.* **10**, 2302249 (2023).
45. Bondarenko, K., Limoge, F., Pedram, K., Gissot, M. & Young, J. C. Enzymatically enhanced ultrastructure expansion microscopy unlocks expansion of in vitro *Toxoplasma gondii* cysts. *mSphere* **9**, e00322–e00324 (2024).
46. Götz, R. et al. Nanoscale imaging of bacterial infections by sphingolipid expansion microscopy. *Nat. Commun.* **11**, 6173 (2020).
47. Trinks, N. et al. Subdiffraction-resolution fluorescence imaging of immunological synapse formation between NK cells and *A. fumigatus* by expansion microscopy. *Commun. Biol.* **4**, 1151 (2021).
48. Lim, Y. et al. Mechanically resolved imaging of bacteria using expansion microscopy. *PLoS Biol.* **17**, e3000268 (2019).
49. White, B. M., Kumar, P., Conwell, A. N., Wu, K. & Baskin, J. M. Lipid expansion microscopy. *J. Am. Chem. Soc.* **144**, 18212–18217 (2022).
50. Asano, S. M. et al. Expansion microscopy: protocols for imaging proteins and RNA in cells and tissues. *Curr. Protoc. Cell Biol.* **80**, e56 (2018).
51. Zhang, C., Kang, J. S., Asano, S. M., Gao, R. & Boyden, E. S. Expansion microscopy for beginners: visualizing microtubules in expanded cultured HeLa cells. *Curr. Protoc. Neurosci.* **92**, e96 (2020).
52. Truckenbrodt, S., Sommer, C., Rizzoli, S. O. & Danzl, J. G. A practical guide to optimization in ×10 expansion microscopy. *Nat. Protoc.* **14**, 832–863 (2019).
53. Mäntylä, E. et al. Iterative immunostaining combined with expansion microscopy and image processing reveals nanoscopic network organization of nuclear lamina. *Mol. Biol. Cell* **34**, br13 (2023).
54. Scalia, C. R. et al. Antigen masking during fixation and embedding, dissected. *J. Histochem. Cytochem.* **65**, 5–20 (2017).
55. Ku, T. et al. Multiplexed and scalable super-resolution imaging of three-dimensional protein localization in size-adjustable tissues. *Nat. Biotechnol.* **34**, 973–981 (2016).
56. Laporte, M. H., Klena, N., Hamel, V. & Guichard, P. Visualizing the native cellular organization by coupling cryofixation with expansion microscopy (Cryo-ExM). *Nat. Methods* **19**, 216–222 (2022).
57. Dahl, R. & Staehelin, L. A. High-pressure freezing for the preservation of biological structure: theory and practice. *J. Electron Microsc. Tech.* **13**, 165–174 (1989).
58. Kakimoto, K., Takekoshi, S., Miyajima, K. & Osamura, R. Y. Hypothesis for the mechanism for heat-induced antigen retrieval occurring on fresh frozen sections without formalin-fixation in immunohistochemistry. *J. Mol. Histol.* **39**, 389–399 (2008).
59. Hubrecht, R. C. & Carter, E. The 3Rs and humane experimental technique: implementing change. *Animals* **9**, 754 (2019).
60. Office for Human Research Protections. Attachment D: FAQ's Terms and Recommendations on Informed Consent and Research Use of Biospecimens. *US Department of Heath and Human Services* https://www.hhs.gov/ohrp/sachrp-committee/recommendations/2011-october-13-letter-attachment-d/index.html (2011).
61. Sun, D. et al. Click-ExM enables expansion microscopy for all biomolecules. *Nat. Methods* **18**, 107–113 (2021).
62. Park, J. et al. Epitope-preserving magnified analysis of proteome (eMAP). *Sci. Adv.* **7**, eabf6589 (2021).
63. Wang, Y. et al. EASI-FISH for thick tissue defines lateral hypothalamus spatio-molecular organization. *Cell* **184**, 6361–6377.e24 (2021).
64. Tsanov, N. et al. smiFISH and FISH-quant — a flexible single RNA detection approach with super-resolution capability. *Nucleic Acids Res.* **44**, e165 (2016).
65. Jetishi, C., Balmer, E. A., Berger, B. M., Faso, C. & Ochsenreiter, T. Expansion of metabolically labelled endocytic organelles and cytoskeletal cell structures in Giardia lamblia using optimised U- ExM protocols. *Microb. Cell* **11**, 198–206 (2024).
66. Shin, T. W. et al. Dense, continuous membrane labeling and expansion microscopy visualization of ultrastructure in tissues. *Nat. Commun.* **16**, 1579 (2025).
67. Park, H.-E. et al. Scalable and isotropic expansion of tissues with simply tunable expansion ratio. *Adv. Sci.* **6**, 1901673 (2019).
68. Yamamoto, T., Tsutsumi, K. & Maeda, S. Green synthesis of hollow structures through the decomposition of azo compounds incorporated inside polystyrene particles. *ACS Omega* **7**, 28556–28560 (2022).
69. Sniegowski, J. A., Phail, M. E. & Wachter, R. M. Maturation efficiency, trypsin sensitivity, and optical properties of Arg96, Glu222, and Gly67 variants of green fluorescent protein. *Biochem. Biophys. Res. Commun.* **332**, 657–663 (2005).
70. Gao, R. et al. Cortical column and whole-brain imaging with molecular contrast and nanoscale resolution. *Science* **363**, eaau8302 (2019).
This work presents a high-throughput imaging pipeline that combines ExM with lattice light-sheet microscopy to map neural circuits across large brain volumes with nanoscale resolution and molecular contrast.
71. Sarkar, D. et al. Revealing nanostructures in brain tissue via protein decrowding by iterative expansion microscopy. *Nat. Biomed. Eng.* **6**, 1057–1073 (2022).
72. Lee, M. Y. et al. Fluorescent labeling of abundant reactive entities (FLARE) for cleared-tissue and super-resolution microscopy. *Nat. Protoc.* **17**, 819–846 (2022).
73. M'Saad, O. & Bewersdorf, J. Light microscopy of proteins in their ultrastructural context. *Nat. Commun.* **11**, 3850 (2020).

74. Shaib, A. H. et al. One-step nanoscale expansion microscopy reveals individual protein shapes. *Nat. Biotechnol.* https://doi.org/10.1038/s41587-024-02431-9 (2024).
This work reports a one-step ExM protocol that achieves ~1-nm effective resolution, enabling the visualization of the shapes of individual proteins.
75. Tavakoli, M. R. et al. Light-microscopy-based connectomic reconstruction of mammalian brain tissue. *Nature* **642**, 398–410 (2025).
76. Grison, M. S. et al. Root expansion microscopy: a robust method for super resolution imaging in *Arabidopsis*. *Plant Cell* **37**, koaf050 (2025).
77. Gallei, M. et al. Super-resolution expansion microscopy in plant roots. *Plant Cell* **37**, koaf006 (2025).
78. Kao, P. & Nodine, M. D. Transcriptional activation of *Arabidopsis* zygotes is required for initial cell divisions. *Sci. Rep.* **9**, 17159 (2019).
79. Jekel, P. A., Weijer, W. J. & Beintema, J. J. Use of endoproteinase Lys-C from *Lysobacter enzymogenes* in protein sequence analysis. *Anal. Biochem.* **134**, 347–354 (1983).
80. Olsen, J. V., Ong, S.-E. & Mann, M. Trypsin cleaves exclusively C-terminal to arginine and lysine residues. *Mol. Cell Proteom.* **3**, 608–614 (2004).
81. van der Hoeven, L. R., Lechner, M., Hernandez-Rollan, C., Batth, T. S. & Olsen, J. V. Comparative analysis of lysine-specific peptidases for optimizing proteomics workflows. *J. Proteome Res.* **25**, 1176–1183 (2026).
82. Yu, C.-C. (J.) et al. Expansion microscopy of *C. elegans*. *eLife* **9**, e46249 (2020).
83. Steib, E. et al. TissUExM enables quantitative ultrastructural analysis in whole vertebrate embryos by expansion microscopy. *Cell Rep. Methods* **2**, 100311 (2022).
84. Chen, L. et al. Applications of super resolution expansion microscopy in yeast. *Front. Phys.* **9**, 650353 (2021).
85. Hinterndorfer, K. et al. Ultrastructure expansion microscopy reveals the cellular architecture of budding and fission yeast. *J. Cell Sci.* **135**, jcs260240 (2022).
86. Reza, M. H. et al. Expansion microscopy reveals characteristic ultrastructural features of pathogenic budding yeast species. *J. Cell Sci*. **137**, jcs262046 (2024).
87. Mikus, F. & Dey, G. in *Schizosaccharomyces pombe*: *Methods and Protocols* (ed. Petreaca, R. C.) 47–59 (Springer, 2025).
88. Huang, K. C., Mukhopadhyay, R., Wen, B., Gitai, Z. & Wingreen, N. S. Cell shape and cell-wall organization in Gram-negative bacteria. *Proc. Natl Acad. Sci. USA* **105**, 19282–19287 (2008).
89. Silhavy, T. J., Kahne, D. & Walker, S. The bacterial cell envelope. *Cold Spring Harb. Perspect. Biol.* **2**, a000414 (2010).
90. Sarfatis, A., Wang, Y., Twumasi-Ankrah, N. & Moffitt, J. R. Highly multiplexed spatial transcriptomics in bacteria. *Science* **387**, eadr0932 (2025).
91. Valdivieso González, D., Jara, J., Almendro-Vedia, V. G., Orgaz, B. & López-Montero, I. Expansion microscopy applied to mono- and dual-species biofilms. *npj Biofilms Microb.* **9**, 1–15 (2023).
92. Saal, K. A. et al. Heat denaturation enables multicolor ×10-STED microscopy. *Sci. Rep.* **13**, 5366 (2023).
93. Amiza, M. A., Khuzma, D., Liew, P. S., Salma Malihah, M. & Sarbon, N. M. Effect of heat treatment and enzymatic protein hydrolysis on the degree of hydrolysis and physicochemical properties of edible bird's nest. *Food Res.* **3**, 664–677 (2019).
94. Kubalová, I. et al. Prospects and limitations of expansion microscopy in chromatin ultrastructure determination. *Chromosome Res.* **28**, 355–368 (2020).
95. Huff, J. The Airyscan detector from ZEISS: confocal imaging with improved signal-to-noise ratio and super-resolution. *Nat. Methods* **12**, i–ii (2015).
96. Schulz, O. et al. Resolution doubling in fluorescence microscopy with confocal spinning-disk image scanning microscopy. *Proc. Natl Acad. Sci. USA* **110**, 21000–21005 (2013).
97. Castello, M. et al. A robust and versatile platform for image scanning microscopy enabling super-resolution FLIM. *Nat. Methods* **16**, 175–178 (2019).
98. Bürgers, J. et al. Light-sheet fluorescence expansion microscopy: fast mapping of neural circuits at super resolution. *Neurophotonics* **6**, 015005 (2019).
99. Pesce, L., Ricci, P., Sportelli, G., Belcari, N. & Sancataldo, G. Expansion and light-sheet microscopy for nanoscale 3D imaging. *Small Methods* **8**, 2301715 (2024).
100. Sanderson, M. J., Smith, I., Parker, I. & Bootman, M. D. Fluorescence microscopy. *Cold Spring Harb. Protoc.* **2014**, pdb.top071795 (2014).
101. Thielhorn, R. et al. Controlled grafting expansion. *Microsc. Angew. Chem. Int. Ed.* **62**, e202302318 (2023).
102. Park, C. E. et al. Super-resolution three-dimensional imaging of actin filaments in cultured cells and the brain via expansion microscopy. *ACS Nano* **14**, 14999–15010 (2020).
103. Pawley, J. (ed.) *Handbook of Biological Confocal Microscopy* (Springer Science & Business Media, 2006).
104. Gao, M. et al. Expansion stimulated emission depletion microscopy (ExSTED). *ACS Nano* **12**, 4178–4185 (2018).
105. Unnersjö-Jess, D. et al. Confocal super-resolution imaging of the glomerular filtration barrier enabled by tissue expansion. *Kidney Int.* **93**, 1008–1013 (2018).
106. Kim, D., Kim, T., Lee, J. & Shim, S.-H. Amplified expansion stimulated emission depletion microscopy. *ChemBioChem* **20**, 1260–1265 (2019).
107. Li, R., Chen, X., Lin, Z., Wang, Y. & Sun, Y. Expansion enhanced nanoscopy. *Nanoscale* **10**, 17552–17556 (2018).
108. Kunz, T. C., Götz, R., Gao, S., Sauer, M. & Kozjak-Pavlovic, V. Using expansion microscopy to visualize and characterize the morphology of mitochondrial cristae. *Front. Cell Dev. Biol.* **8**, 617 (2020).
109. Halpern, A. R., Alas, G. C. M., Chozinski, T. J., Paredez, A. R. & Vaughan, J. C. Hybrid structured illumination expansion microscopy reveals microbial cytoskeleton organization. *ACS Nano* **11**, 12677–12686 (2017).
110. Wang, Y. et al. Combined expansion microscopy with structured illumination microscopy for analyzing protein complexes. *Nat. Protoc.* **13**, 1869–1895 (2018).
111. Zwettler, F. U. et al. Tracking down the molecular architecture of the synaptonemal complex by expansion microscopy. *Nat. Commun.* **11**, 3222 (2020).
112. Cahoon, C. K. et al. Superresolution expansion microscopy reveals the three-dimensional organization of the *Drosophila* synaptonemal complex. *Proc. Natl Acad. Sci. USA* **114**, E6857–E6866 (2017).
113. Shi, X. et al. Label-retention expansion microscopy. *J. Cell Biol.* **220**, e202105067 (2021).
114. Kuang, W., Xin, B., Huang, Z.-L. & Shi, B. A labeling strategy with effective preservation of fluorophores for expansion single-molecule localization microscopy (Ex-SMLM). *Analyst* **147**, 139–146 (2021).
115. Zwettler, F. U. et al. Molecular resolution imaging by post-labeling expansion single-molecule localization microscopy (Ex-SMLM). *Nat. Commun.* **11**, 3388 (2020).
116. Vojnovic, I., Caspari, O. D., Hoşkan, M. A. & Endesfelder, U. Combining single-molecule and expansion microscopy in fission yeast to visualize protein structures at the nanostructural level. *Open Biol.* **14**, 230414 (2024).
117. Xu, H. et al. Molecular organization of mammalian meiotic chromosome axis revealed by expansion STORM microscopy. *Proc. Natl Acad. Sci. USA* **116**, 18423–18428 (2019).
118. Klimas, A., Gallagher, B. & Zhao, Y. Basics of expansion microscopy. *Curr. Protoc. Cytom.* **91**, e67 (2019).
119. Gao, R., Asano, S. M. & Boyden, E. S. Q&A: expansion microscopy. *BMC Biol.* **15**, 50 (2017).
120. Shen, F. Y. et al. Light microscopy based approach for mapping connectivity with molecular specificity. *Nat. Commun.* **11**, 4632 (2020).
121. Schindelin, J. et al. Fiji: an open-source platform for biological-image analysis. *Nat. Methods* **9**, 676–682 (2012).
122. Wang, U.-T. T. et al. Protein and lipid expansion microscopy with trypsin and tyramide signal amplification for 3D imaging. *Sci. Rep.* **13**, 21922 (2023).
123. Hörl, D. et al. BigStitcher: reconstructing high-resolution image datasets of cleared and expanded samples. *Nat. Methods* **16**, 870–874 (2019).
124. Loi, J., Ghone, D., Qu, X. & Suzuki, A. 3D-Aligner: advanced computational tool for correcting image distortion in expansion microscopy. *Commun. Biol.* **7**, 1–9 (2024).
125. Fixstars announces the release of expansion microscopy studio including the world's fastest deconvolution software. *Fixstars Corporation* https://www.fixstars.com/en/news/852 (2018).
126. Parmar, J. J., Woringer, M. & Zimmer, C. How the genome folds: the biophysics of four-dimensional chromatin organization. *Annu. Rev. Biophys.* **48**, 231–253 (2019).
127. Strahl, B. D. & Allis, C. D. The language of covalent histone modifications. *Nature* **403**, 41–45 (2000).
128. Jenuwein, T. & Allis, C. D. Translating the histone code. *Science* **293**, 1074–1080 (2001).
129. Bannister, A. J. & Kouzarides, T. Regulation of chromatin by histone modifications. *Cell Res.* **21**, 381–395 (2011).
130. Henninger, J. E. & Young, R. A. An RNA-centric view of transcription and genome organization. *Mol. Cell* **84**, 3627–3643 (2024).
131. Vorobjev, I. A. & YuS, C. Centrioles in the cell cycle. I. Epithelial cells. *J. Cell Biol.* **93**, 938–949 (1982).
132. Laporte, M. H. et al. Time-series reconstruction of the molecular architecture of human centriole assembly. *Cell* **187**, 2158–2174.e19 (2024).
133. Matias, V. R. F. & Beveridge, T. J. Native cell wall organization shown by cryo-electron microscopy confirms the existence of a periplasmic space in *Staphylococcus aureus*. *J. Bacteriol.* **188**, 1011–1021 (2006).
134. Goldsmith, C. S. & Miller, S. E. Modern uses of electron microscopy for detection of viruses. *Clin. Microbiol. Rev.* **22**, 552–563 (2009).
135. Schirra, R. T. Jr. & Zhang, P. Correlative fluorescence and electron microscopy. *Curr. Protoc. Cytom.* **70**, 12.36.1–12.36.10 (2014).
136. Jennings, P. C., Cox, G. C., Monahan, L. G. & Harry, E. J. Super-resolution imaging of the bacterial cytokinetic protein FtsZ. *Micron* **42**, 336–341 (2011).
137. Coltharp, C. & Xiao, J. Superresolution microscopy for microbiology. *Cell. Microbiol.* **14**, 1808–1818 (2012).
138. Schermelleh, L., Heintzmann, R. & Leonhardt, H. A guide to super-resolution fluorescence microscopy. *J. Cell Biol.* **190**, 165–175 (2010).
139. Dong, P.-T., Shi, W., He, X. & Borisy, G. G. Adhesive interactions within microbial consortia can be differentiated at the single-cell level through expansion microscopy. *Proc. Natl Acad. Sci. USA* **121**, e2411617121 (2024).
140. Liffner, B. et al. Atlas of *Plasmodium falciparum* intraerythrocytic development using expansion microscopy. *eLife* **12**, RP88088 (2023).
141. Ren, B. et al. Architecture of the *Toxoplasma gondii* apical polar ring and its role in gliding motility and invasion. *Proc. Natl Acad. Sci. USA* **121**, e2416602121 (2024).
142. Qian, P. et al. Apical anchorage and stabilization of subpellicular microtubules by apical polar ring ensures *Plasmodium* ookinete infection in mosquito. *Nat. Commun.* **13**, 7465 (2022).
143. Guevara, R. B., Fox, B. A., Falla, A. & Bzik, D. J. *Toxoplasma gondii* intravacuolar-network-associated dense granule proteins regulate maturation of the cyst matrix and cyst wall. *mSphere* https://doi.org/10.1128/msphere.00487-19 (2019).
144. Bertiaux, E. et al. Expansion microscopy provides new insights into the cytoskeleton of malaria parasites including the conservation of a conoid. *PLoS Biol.* **19**, e3001020 (2021).

145. Bartholomäus, A. et al. Bacteria differently regulate mRNA abundance to specifically respond to various stresses. *Philos. Trans. R. Soc. Math. Phys. Eng. Sci.* **374**, 20150069 (2016).
146. Wassie, A. T., Zhao, Y. & Boyden, E. S. Expansion microscopy: principles and uses in biological research. *Nat. Methods* **16**, 33–41 (2019).
147. Goodwin, D. R. et al. Expansion sequencing of RNA barcoded neurons in the mammalian brain: progress and implications for molecularly annotated connectomics. Preprint at *bioRxiv* https://doi.org/10.1101/2022.07.31.502046 (2022).
148. Eng, C.-H. L. et al. Transcriptome-scale super-resolved imaging in tissues by RNA seqFISH+. *Nature* **568**, 235–239 (2019).
149. Sneve, M. A. & Piatkevich, K. D. Towards a comprehensive optical connectome at single synapse resolution via expansion microscopy. *Front. Synaptic Neurosci.* **13**, 754814 (2022).
150. Akins, M. R., Berk-Rauch, H. E. & Fallon, J. Presynaptic translation: stepping out of the postsynaptic shadow. *Front. Neural Circuits* **3**, 17 (2009).
151. Alvarez, J., Giuditta, A. & Koenig, E. Protein synthesis in axons and terminals: significance for maintenance, plasticity and regulation of phenotype: with a critique of slow transport theory. *Prog. Neurobiol.* **62**, 1–62 (2000).
152. Kleiman, R., Banker, G. & Steward, O. Development of subcellular mRNA compartmentation in hippocampal neurons in culture. *J. Neurosci.* **14**, 1130–1140 (1994).
153. Loh, K. H. et al. Proteomic analysis of unbounded cellular compartments: synaptic clefts. *Cell* **166**, 1295–1307.e21 (2016).
154. Bassell, G. J. et al. Sorting of β-actin mRNA and protein to neurites and growth cones in culture. *J. Neurosci.* **18**, 251–265 (1998).
155. Scarnati, M. S., Kataria, R., Biswas, M. & Paradiso, K. G. Active presynaptic ribosomes in the mammalian brain, and altered transmitter release after protein synthesis inhibition. *eLife* **7**, e36697 (2018).
156. Terasaki, M. Axonal endoplasmic reticulum is very narrow. *J. Cell Sci.* **131**, jcs210450 (2018).
157. Lichtman, J. W. & Denk, W. The big and the small: challenges of imaging the brain's circuits. *Science* **334**, 618–623 (2011).
158. Steib, E., Vagena-Pantoula, C. & Vermot, J. TissUExM protocol for ultrastructure expansion microscopy of zebrafish larvae and mouse embryos. *STAR Protoc.* **4**, 102257 (2023).
159. Cai, D., Cohen, K. B., Luo, T., Lichtman, J. W. & Sanes, J. R. Improved tools for the Brainbow toolbox. *Nat. Methods* **10**, 540–547 (2013).
160. M'Saad, O. et al. All-optical visualization of specific molecules in the ultrastructural context of brain tissue. *Nat. Biotechnol.* https://doi.org/10.1038/s41587-025-02905-4 (2025).
161. Arsenijevic, Y. et al. Fine-tuning FAM161A gene augmentation therapy to restore retinal function. *EMBO Mol. Med.* **16**, 805–822 (2024).
162. Klughammer, J. et al. A multi-modal single-cell and spatial expression map of metastatic breast cancer biopsies across clinicopathological features. *Nat. Med.* **30**, 3236–3249 (2024).
163. Liu, Y. & Xu, J. High-resolution microscopy for imaging cancer pathobiology. *Curr. Pathobiol. Rep.* **7**, 85–96 (2019).
164. Liu, Y., Uttam, S., Alexandrov, S. & Bista, R. K. Investigation of nanoscale structural alterations of cell nucleus as an early sign of cancer. *BMC Biophys.* **7**, 1 (2014).
165. Creech, M. K., Wang, J., Nan, X. & Gibbs, S. L. Superresolution imaging of clinical formalin fixed paraffin embedded breast cancer with single molecule localization microscopy. *Sci. Rep.* **7**, 40766 (2017).
166. Mousavikhamene, Z., Sykora, D. J., Mrksich, M. & Bagheri, N. Morphological features of single cells enable accurate automated classification of cancer from non-cancer cell lines. *Sci. Rep.* **11**, 24375 (2021).
167. Ilgen, P. et al. STED super-resolution microscopy of clinical paraffin-embedded human rectal cancer tissue. *PLoS ONE* **9**, e101563 (2014).
168. Xu, J. et al. Super-resolution imaging reveals the evolution of higher-order chromatin folding in early carcinogenesis. *Nat. Commun.* **11**, 1899 (2020).
169. Kufukihara, R. et al. Hybridisation chain reaction-based visualisation and screening for lncRNA profiles in clear-cell renal-cell carcinoma. *Br. J. Cancer* **127**, 1133–1141 (2022).
170. Kubala, J. M. et al. NDUFA4L2 reduces mitochondrial respiration resulting in defective lysosomal trafficking in clear cell renal cell carcinoma. *Cancer Biol. Ther.* **24**, 2170669 (2023).
171. Cairns, R. A., Papandreou, I., Sutphin, P. D. & Denko, N. C. Metabolic targeting of hypoxia and HIF1 in solid tumors can enhance cytotoxic chemotherapy. *Proc. Natl Acad. Sci. USA* **104**, 9445–9450 (2007).
172. Ma, S. et al. Hypoxia induces HIF1α-dependent epigenetic vulnerability in triple negative breast cancer to confer immune effector dysfunction and resistance to anti-PD-1 immunotherapy. *Nat. Commun.* **13**, 4118 (2022).
173. Krummel, M. F. & Cahalan, M. D. The immunological synapse: a dynamic platform for local signaling. *J. Clin. Immunol.* **30**, 364–372 (2010).
174. Lemaître, F. et al. Unveiling the molecular architecture of T cells and immune synapses with cryo-expansion microscopy. Preprint at *bioRxiv* https://doi.org/10.1101/2025.04.15.648816 (2025).
175. Kumar-Singh, S. et al. Dense-core plaques in Tg2576 and PSAPP mouse models of Alzheimer's disease are centered on vessel walls. *Am. J. Pathol.* **167**, 527–543 (2005).
176. Johansson, B. et al. The interwoven fibril-like structure of amyloid-beta plaques in mouse brain tissue visualized using super-resolution STED microscopy. *Cell Biosci.* **13**, 142 (2023).
177. Hyde, V. R. et al. Anti-herpetic tau preserves neurons via the cGAS–STING–TBK1 pathway in Alzheimer's disease. *Cell Rep.* **44**, 115109 (2025).
178. Elliott, A. D. Confocal microscopy: principles and modern practices. *Curr. Protoc. Cytom.* **92**, e68 (2020).
179. Louvel, V. et al. iU-ExM: nanoscopy of organelles and tissues with iterative ultrastructure expansion microscopy. *Nat. Commun.* **14**, 7893 (2023).
180. Morgan, K. J. et al. Visualizing nuclear pore complex plasticity with pan-expansion microscopy. *J. Cell Biol.* **224**, e202409120 (2025).
181. Damstra, H. G. J. et al. GelMap: intrinsic calibration and deformation mapping for expansion microscopy. *Nat. Methods* **20**, 1573–1580 (2023).
182. Petrich, A. et al. Expanding insights: harnessing expansion microscopy for super-resolution analysis of HIV-1–cell interactions. *Viruses* **16**, 1610 (2024).
183. Wilkinson, M. D. et al. The FAIR guiding principles for scientific data management and stewardship. *Sci. Data* **3**, 160018 (2016).
184. Karagiannis, E. D. & Boyden, E. S. Expansion microscopy: development and neuroscience applications. *Curr. Opin. Neurobiol.* **50**, 56–63 (2018).
185. Wang, Y. et al. Multiplexed in situ protein imaging using DNA-barcoded antibodies with extended hybridization chain reactions. *Nucleic Acids Res.* **52**, e71 (2024).
186. Saka, S. K. et al. Immuno-SABER enables highly multiplexed and amplified protein imaging in tissues. *Nat. Biotechnol.* **37**, 1080–1090 (2019).
187. Lin, R. et al. A hybridization-chain-reaction-based method for amplifying immunosignals. *Nat. Methods* **15**, 275–278 (2018).
188. Cho, I. & Chang, J.-B. Simultaneous expansion microscopy imaging of proteins and mRNAs via dual-ExM. *Sci. Rep.* **12**, 3360 (2022).
189. Odenwald, J. et al. Detection of TurboID fusion proteins by fluorescent streptavidin outcompetes antibody signals and visualises targets not accessible to antibodies. *eLife* **13**, RP95028 (2024).
190. Hecht, A. M., Duplessix, R. & Geissler, E. Structural inhomogeneities in the range 2.5-2500 ANG. in polyacrylamide gels. *Macromolecules* **18**, 2167–2173 (1985).
191. Calvet, D., Wong, J. Y. & Giasson, S. Rheological monitoring of polyacrylamide gelation: importance of cross-link density and temperature. *Macromolecules* **37**, 7762–7771 (2004).
192. Di Lorenzo, F. & Seiffert, S. Nanostructural heterogeneity in polymer networks and gels. *Polym. Chem.* **6**, 5515–5528 (2015).
193. Cohen, Y., Ramon, O., Kopelman, I. J. & Mizrahi, S. Characterization of inhomogeneous polyacrylamide hydrogels. *J. Polym. Sci. Part B Polym. Phys.* **30**, 1055–1067 (1992).
194. Park, H. H., Choi, A. A. & Xu, K. Size-dependent suppression of molecular diffusivity in expandable hydrogels: a single-molecule study. *J. Phys. Chem. B* **127**, 3333–3339 (2023).
195. Shi, L. et al. Super-resolution vibrational imaging using expansion stimulated Raman scattering microscopy. *Adv. Sci.* **9**, 2200315 (2022).
196. Qian, C. et al. Super-resolution label-free volumetric vibrational imaging. *Nat. Commun.* **12**, 3648 (2021).
197. Lin, L.-E., Miao, K., Qian, C. & Wei, L. High spatial-resolution imaging of label-free in vivo protein aggregates by VISTA. *Analyst* **146**, 4135–4145 (2021).
198. Lee, H., Yu, C.-C., Boyden, E. S., Zhuang, X. & Kosuri, P. Tetra-gel enables superior accuracy in combined super-resolution imaging and expansion microscopy. *Sci. Rep.* **11**, 16944 (2021).
199. Park, Y.-G. et al. Protection of tissue physicochemical properties using polyfunctional crosslinkers. *Nat. Biotechnol.* **37**, 73–83 (2019).
200. Seehra, R. S. et al. Geometry-preserving expansion microscopy microplates enable high-fidelity nanoscale distortion mapping. *Cell Rep. Phys. Sci.* **4**, 101719 (2023).
201. Day, J. H. et al. High-throughput expansion microscopy enables scalable super-resolution imaging. *eLife* **13**, RP96025 (2024).
202. Drelich, L. et al. Toward high spatially resolved proteomics using expansion microscopy. *Anal. Chem.* **93**, 12195–12203 (2021).
203. Li, L. et al. Spatially resolved proteomics via tissue expansion. *Nat. Commun.* **13**, 7242 (2022).
204. Zhang, H. et al. TEMI: tissue-expansion mass-spectrometry imaging. *Nat. Methods* **22**, 1051–1058 (2025).
205. Chan, Y. H. et al. Gel-assisted mass spectrometry imaging enables sub-micrometer spatial lipidomics. *Nat. Commun.* **15**, 5036 (2024).
206. Bai, Y. et al. Expanded vacuum-stable gels for multiplexed high-resolution spatial histopathology. *Nat. Commun.* **14**, 4013 (2023).
207. Wang, F. et al. iPEX enables micrometre-resolution deep spatial proteomics via tissue expansion. *Nature* https://doi.org/10.1038/s41586-025-09734-0 (2025).
208. Liffner, B., Silva, T. L. A., Vega-Rodriguez, J. & Absalon, S. Mosquito tissue ultrastructure-expansion microscopy (MoTissU-ExM) enables ultrastructural and anatomical analysis of malaria parasites and their mosquito. *BMC Methods* **1**, 13 (2024).
209. Mikus, F. et al. Charting the landscape of cytoskeletal diversity in microbial eukaryotes. *Cell* https://doi.org/10.1016/j.cell.2025.09.027 (2025).
210. Glaser, A. et al. Expansion-assisted selective plane illumination microscopy for nanoscale imaging of centimeter-scale tissues. *eLife* **12**, RP91979 (2024).
211. Park, J. et al. Integrated platform for multiscale molecular imaging and phenotyping of the human brain. *Science* **384**, eadh9979 (2024).
212. Günay, K. A. et al. Photo-expansion microscopy enables super-resolution imaging of cells embedded in 3D hydrogels. *Nat. Mater.* **22**, 777–785 (2023).

Acknowledgements

E.S.B. acknowledges funding from Lisa Yang, Good Ventures and Open Philanthropy, Schmidt Futures, John Doerr, HHMI, Tom Stocky and Avni Shah, Kathleen Octavio, ERC Synergy grant no. 835102 and NIH 1R01EB024261, 1R01AG070831 and R01AG087374. Y.Z. acknowledges funding from NIH grants RF1 MH129267, R01 EB035890, 1AY2AX000056 and R01 CA301488 and the Eberly Family Professorship. The authors thank M. Gao, J. Jeffrey and R. Pratt for critical reading of the manuscript and providing excellent feedback.

Author contributions
The authors contributed equally to all aspects of the article.

Competing interests
E.S.B. is co-founder of a company seeking to deploy applications of ExM-related technologies. Y.Z. is co-founder of a company disseminating Magnify kits and service. E.S.B., Y.Z. and R.X. are inventors on multiple patents in the space of expansion microscopy. H.V.V. declares no competing interests.

Additional information
Supplementary information The online version contains supplementary material available at https://doi.org/10.1038/s43586-026-00480-9.

Peer review information *Nature Reviews Methods Primers* thanks the anonymous reviewers for their contribution to the peer review of this work.

nature reviews methods primers

https://doi.org/10.1038/s43586-026-00480-9

Supplementary information

Expansion microscopy

In the format provided by the authors and unedited

Supplementary information

Expansion Microscopy

Ha V. Vo[1§], Rong Xu[1§], Edward S. Boyden[2,3,4,5,6,10,11*], Yongxin Zhao[1,7,8,9*]

[1] Department of Biological Sciences, Carnegie Mellon University, Pittsburgh, PA, USA.
[2] Department of Brain and Cognitive Sciences, Massachusetts Institute of Technology, Cambridge, MA, USA.
[3] Department of Biological Engineering, Massachusetts Institute of Technology, Cambridge, MA, USA.
[4] McGovern Institute, Massachusetts Institute of Technology, Cambridge, MA, USA.
[5] Koch Institute, Massachusetts Institute of Technology, Cambridge, MA, USA.
[6] Center for Neurobiological Engineering, Massachusetts Institute of Technology, Cambridge, MA, USA.
[7] Carnegie Mellon Neuroscience Institute, Pittsburgh, PA, USA.
[8] Department of Biomedical Engineering, Carnegie Mellon University, Pittsburgh, PA, USA.
[9] Viron Molecular Medicine Institute, Boston, MA, USA.

[10] Howard Hughes Medical Institute, Cambridge, MA, USA.

[11] K. Lisa Yang Center for Bionics, and Yang Tan Collective, MIT, Cambridge, MA, USA.

[§]These authors contributed equally to the work

*Corresponding authors: edboyden@mit.edu and yongxinz@andrew.cmu.edu

Supplementary Table 1. Characteristics of some foundational and/or commonly used ExM protocols

Acronym (ranked in chronological order)	Anchoring strategy	Retained molecules	Applicable tissue types	Fixation Prior to Processing	Softening method	Staining order	Expansion factor	Achievable resolution[1]	Notes
ExM[1]	Indirect (via trifunctional oligos)	No endogenous molecules anchored	Cultured cells, brain tissues	PFA	Proteinase K	Pre-expansion	~4.5×	~70 nm	The foundational protocol that introduced the ExM principle.
MA-NHS ExM[2]	Direct (via MA-NHS)	Proteins and DNA[2]	Cultured cells, various tissues	PFA, GA (low level, e.g., 0.1%)	Proteinase K	Pre-expansion	~4.5×	~70 nm	Provides an amine-reactive anchoring alternative to Acryloyl-X.
proExM[3]	Direct (via Acryloyl-X)	Proteins and DNA	Cultured cells, various tissues	PFA	Proteinase K LysC	Pre-expansion	~4.5×	~70 nm	Directly anchoring proteins to the polymer hydrogel
MAP[4]	Direct (via acrylamide + PFA)	Proteins	Cultured cells, tissues	PFA	Heat denaturation	Post-expansion	~4×	~70 nm	Allow post-expansion labeling
ExFISH[5]	Direct (via LabelX)	RNA and proteins	Cultured cells, brain tissues	PFA	Proteinase K	Post-expansion	~4.5×	~70 nm	The first protocol specifically designed for anchoring and imaging RNA molecules

ExPath[6]	Direct (via Acryloyl-X)	Proteins and DNA	Normal and pathological (e.g., FFPE) tissues	Formalin or cold acetone/methanol fixation	Proteinase K	Pre-expansion	~4.5×	~70 nm	Designed for expanding archival clinical specimens
iExM[7]	Indirect (via DNA oligonucleotides with 5' acrydite moieties)	No endogenous molecules anchored	Cultured cells, and brain tissues	PFA	Proteinase K	Pre-expansion	~16-20x	~20 nm	Achieves high expansion factors (~16-20x) through an iterative process of forming a second swellable hydrogel within the first expanded sample.
X10 ExM[8]	Direct (via Acryloyl-X or MA-NHS)	Proteins and DNA	Cultured cells	PFA, GA (low level, e.g., 0.1%)	Proteinase K	Pre-expansion	~10×	~25 nm	A single-step protocol for achieving high (~10x) expansion
U-ExM[9]	Direct (via acrylamide + PFA)	Proteins and DNA	Cultured cells	PFA with acrylamide, PFA and methanol	Heat denaturation	Post-expansion	~4.5×	~70 nm	A modified MAP protocol, optimized for preserving fine ultrastructural details of protein complexes.
ExCel[10]	Direct (via Acryloyl-X)	Proteins and RNAs	*C. elegans*	PFA	Proteinase K and collagenase	Pre-expansion	~3.5x	~75 nm	Expands *C. elegans'* tough cuticle
pan-ExM[11]	Direct (via acrylamide + PFA)	Proteins and DNA	Cultured cells	PFA with acrylamide, PFA and GA	Heat Denaturation	Post-expansion	~13-21x	~25 nm	Uses an iterative expansion strategy and a pan-protein stain to visualize ultrastructure, providing EM-like context.

Click-ExM[12]	Direct (via Acryloyl-X or GA)	Proteins, nucleic acids, lipids, and glycans	Cultured cells	PFA	Proteinase K	Pre-expansion (via clickable fluorescent probes)	~4.5×	~70 nm	Allows metabolic labeling via bioorthogonal chemistry
eMAP[13]	Indirect (via physically trapping of peptide chains)	Proteins and DNA	Cultured cells, tissues	No anchoring	Heat denaturation	Post-expansion	~4×	~70 nm	Allow post-expansion labeling
LR-ExM[14]	Indirect (via customized probes)	Proteins and DNA	Cultured cells	PFA	Proteinase K	Pre-expansion	~4.5×	~70 nm	Uses customized linkers designed for improved label retention during processing
TREx[15]	Direct (via Acryloyl-X)	Proteins and DNA	Cultured cells, brain tissues	PFA	Proteinase K	Pre-expansion	~10×	~25 nm	One step 10× expansion on mouse brain tissue sections
LExM[16]	Direct (via metabolically modifying endogenous lipid molecules)	Lipids	Cultured cells, brain tissues	PFA	Proteinase K	Pre-expansion	~4-6×	~60-70 nm	Allows simultaneous metabolic labeling and anchoring of phospholipids to the hydrogel via bioorthogonal chemistry
ExR[17]	Direct (via PFA with acrylamide)	Proteins	Cultured cells and brain tissues	PFA with acrylamide	Heat Denaturation	Post-expansion	~15-20×	~20 nm	Uses an iterative re-embedding strategy to achieve high expansion while preserving biomolecules for post-expansion staining.

Magnify[18]	Direct (via methacrolein) Concurrent anchoring	Proteins, lipids, nucleic acids	Cultured cells, PFA-fixed tissues, FFPE, organoids	PFA and formalin	Heat denaturation	Post-expansion	Up to 11×	~28 nm	A broad-spectrum, concurrent anchoring strategy for retaining multiple biomolecule types.
MicroMagnify[19]	Direct (via methacrolein) Concurrent anchoring	Proteins, lipids, nucleic acids	Cultured cells, tissues, FFPE, organoids, bacteria	PFA and formalin	Heat denaturation Cell wall digestion	Post-expansion	Up to 11×	~28 nm	Adapts the Magnify chemistry and cell wall digestion for pathogen-infected cells and tissues.
iU-ExM[20]	Direct (via PFA with acrylamide)	Proteins and RNA	Cultured cells, and retina tissues	PFA with acrylamide and GA or methanol	Heat Denaturation	Post-expansion	~16×	~10-20 nm	Achieves high expansion factors by combining U-ExM with iExM
Cryo-ExM[21]	Direct (via acrylamide + PFA)	Proteins and DNA	Cultured cells	freeze-substitution with PFA with acrylamide	Heat denaturation	Post-expansion	~4.5×	~70 nm	Couples cryo-fixation with ExM to preserve native ultrastructure.
uniExM[22]	Direct (via epoxide)	Proteins and RNAs	Cultured cells and tissues	PFA	Proteinase K SDS	Pre-expansion or post-expansion	~4.5×	~70 nm	New class of anchoring simplifies multiplexed imaging of proteins and RNAs

20ExM[23]	Direct (via N-Acryloxysuccinimide)	Proteins and DNA	Cultured cells and brain tissues	PFA	Heat LysC/trypsin	Pre-expansion or post-expansion	~ 20×	<20 nm	Single-step 20× expansion
dExPath[24]	Direct (via Acryloyl-X)	Proteins and DNA	Normal and pathological brain tissues	Formalin	Heat denaturation	Post-expansion	~4×	~70 nm	A variant of ExPath that uses heat-denaturation method to improve immunofluorescence in pathological specimens
umExM[25]	Indirect (via custom lipophilic probe)	Lipids	Brain tissues	PFA and calcium chloride	Proteinase K	Pre-expansion or post-expansion (via customized membrane labeling probes)	~ 4-5×	~60 nm	Designed to enable dense labeling of lipid membranes before expansion
Whole-body ExM[26]	Direct (via Acryloyl-X)	Proteins	Whole mouse embryos	PFA	Proteinase K and collagenase	Pre-expansion	~ 4×	Up to ~90 nm	Designed for expansion of whole organism, focusing on digestion of connective tissues

Note:

[1]With a diffraction limited confocal microscope, 600 nm emission and NA 1.2 water immersion objective, the diffraction limit is ~305 nm.

[2]Due to its extremely large size and entanglement within the polymer network, macromolecular DNA is typically entrapped efficiently by most standard ExM methods, even those without a dedicated covalent nucleic acid anchoring chemistry.

PFA: paraformaldehyde; FA: formaldehyde; GA: glutaraldehyde; MA-NHS: Methacrylic acid N-hydroxysuccinimide ester; FFPE: formalin-fixed paraffin-embedded; SDS: Sodium dodecyl sulfate.

Supplementary Table 2. Representative sample types successfully expanded by ExM methods.

Specimen Types	Examples	Typical Scale of tissues	FP Compatible?	Examples of Applied Protocols	Refs
Cultured Cells	HeLa, HEK293, Primary culture neurons, etc.	Monolayer	Yes	Universally compatible (e.g., proExM, U-ExM, MAP, TREx, X10, ExR, Magnify, 20ExM, etc.)	Validated in the vast majority of ExM publications. See refs [3,4,8,9,15,17,18,23]
Organoids	Human cerebral, lung, airway, etc.	0.3-2 mm	Yes	Magnify,, iPEX, PhASE-ExM	[18,26,27]
Mouse Brain (Slices)	PFA-fixed mouse brain sections	30–200 μm	Yes	Universally compatible (e.g., proExM, U-ExM, MAP, TREx, X10, ExR, Magnify, 20ExM, etc.)	Validated in the vast majority of ExM publications. See refs [3,4,8,9,15,17,18,23]
Mouse Brain (Whole)	Intact organ	cm scale	Yes	Whole-body ExM, ExASPIM	[26,28]
Mouse Organs (Slices)	Kidney, liver, lung	10–100 μm	Yes	proExM, MAP, Magnify	[3,4,18]

Mouse Embryo	E12–E14	Whole (mm scale)	Yes	TissUExM, Whole-body ExM	[26,29]
Human FFPE	Brain (Alzheimer's, glioma), kidney, liver, lung, prostate, colon, pancreas, breast, uterus, ovary, placenta, thymus, thyroid biopsies	5–50 µm	No	ExPath, rExPath, dExPath, Magnify, ExSRRF	[6,18,24,30,31]
Nematodes	*Caenorhabditis elegans*	Whole (~1 mm)	Yes	ExCel	[10]
Insects (dissected)	*Drosophila melanogaster* brain	Whole brain, wings	Yes	ExLLSM, TissUExM	[29,32]
Zebrafish	Embryo / Larvae	Whole (mm scale)	Yes	TissUExM, proExM	[3,29]
Plants	*Arabidopsis thaliana* roots and seeds	Whole root	Yes	PlantEx, ROOT-ExM	[33,34]
Bacteria	*Escherichia coli, Staphylococcus aureus*	Cell / Infected Cell	Yes	µExM, MicroMagnify	[19,35]
Fungi	*Aspergillus fumigatus*, *Candida albicans*	Cell / Biofilm / Tissue	Yes	ExM with Glucanex, MicroMagnify	[19,36]

Parasites	*Plasmodium*, *Toxoplasma*, *Acanthamoeba*	Cell / Tissue/Cyst	Yes	U-ExM, MicroMagnify	[19,37]

Supplementary Table 3. Common fluorophores in the pre-expansion staining workflow

Type	Excitation Maxima (nm)	Emission Maxima (nm)	References
Fluorescent Dyes			
CF405M	408	452	[3]
Alexa488	495	519	[1,3]
Alexa546	556	573	[3]
Alexa555	555	565	[12]
SYBR Gold	495	537	[2]
Atto565	562	589	[1]
Alexa594	590	617	[3]
CF633	630	650	[3]
Atto647N	644	669	[1,3]
Fluorescent Proteins			
EBFP2	383	448	[3]
mTagBFP2	399	454	[3]
mTurquoise2	434	474	[3]
mCerulean3	433	475	[3]
ECFP	434	477	[3]
mTFP1	462	492	[3]
mEmerald	487	509	[3]

EGFP	489	509	[3]
mClover	505	515	[3]
EYFP	514	527	[3]
mVenus	515	528	[3]
mCitrine	516	529	[3]
mOrange2	549	565	[3]
LSSmOrange	437	572	[3]
tdTomato	554	581	[3]
mRuby2	559	600	[3]
mCherry	587	610	[3]
mKate2	588	633	[3]
mCardinal	604	659	[3]

References

1. Chen, F., Tillberg, P. W. & Boyden, E. S. Expansion microscopy. *Science* **347**, 543–548 (2015).
2. Chozinski, T. J. *et al.* Expansion microscopy with conventional antibodies and fluorescent proteins. *Nat. Methods* **13**, 485–488 (2016).
3. Tillberg, P. W. *et al.* Protein-retention expansion microscopy of cells and tissues labeled using standard fluorescent proteins and antibodies. *Nat. Biotechnol.* **34**, 987–992 (2016).
4. Ku, T. *et al.* Multiplexed and scalable super-resolution imaging of three-dimensional protein localization in size-adjustable tissues. *Nat. Biotechnol.* **34**, 973–981 (2016).
5. Chen, F. *et al.* Nanoscale imaging of RNA with expansion microscopy. *Nat. Methods* **13**, 679–684 (2016).
6. Zhao, Y. *et al.* Nanoscale imaging of clinical specimens using pathology-optimized expansion microscopy. *Nat. Biotechnol.* **35**, 757–764 (2017).
7. Chang, J.-B. *et al.* Iterative expansion microscopy. *Nat. Methods* **14**, 593–599 (2017).
8. Truckenbrodt, S. *et al.* X10 expansion microscopy enables 25-nm resolution on conventional microscopes. *EMBO Rep.* **19**, e45836 (2018).
9. Gambarotto, D. *et al.* Imaging cellular ultrastructures using expansion microscopy (U-ExM). *Nat. Methods* **16**, 71–74 (2019).
10. Yu, C.-C. (Jay) *et al.* Expansion microscopy of C. elegans. *eLife* **9**, e46249 (2020).
11. M'Saad, O. & Bewersdorf, J. Light microscopy of proteins in their ultrastructural context. *Nat. Commun.* **11**, 3850 (2020).
12. Sun, D. *et al.* Click-ExM enables expansion microscopy for all biomolecules. *Nat. Methods* **18**, 107–113 (2021).
13. Park, J. *et al.* Epitope-preserving magnified analysis of proteome (eMAP). *Sci. Adv.* **7**, eabf6589 (2021).
14. Shi, X. *et al.* Label-retention expansion microscopy. *J. Cell Biol.* **220**, e202105067 (2021).

15. Damstra, H. G. *et al.* Visualizing cellular and tissue ultrastructure using Ten-fold Robust Expansion Microscopy (TREx). *eLife* **11**, e73775 (2022).

16. White, B. M., Kumar, P., Conwell, A. N., Wu, K. & Baskin, J. M. Lipid Expansion Microscopy. *J. Am. Chem. Soc.* **144**, 18212–18217 (2022).

17. Sarkar, D. *et al.* Revealing nanostructures in brain tissue via protein decrowding by iterative expansion microscopy. *Nat. Biomed. Eng.* **6**, 1057–1073 (2022).

18. Klimas, A. *et al.* Magnify is a universal molecular anchoring strategy for expansion microscopy. *Nat. Biotechnol.* **41**, 858–869 (2023).

19. Cheng, Z. *et al.* MicroMagnify: A Multiplexed Expansion Microscopy Method for Pathogens and Infected Tissues. *Adv. Sci.* **10**, 2302249 (2023).

20. Louvel, V. *et al.* iU-ExM: nanoscopy of organelles and tissues with iterative ultrastructure expansion microscopy. *Nat. Commun.* **14**, 7893 (2023).

21. Laporte, M. H., Klena, N., Hamel, V. & Guichard, P. Visualizing the native cellular organization by coupling cryofixation with expansion microscopy (Cryo-ExM). *Nat. Methods* **19**, 216–222 (2022).

22. Cui, Y. *et al.* Expansion microscopy using a single anchor molecule for high-yield multiplexed imaging of proteins and RNAs. *PLOS ONE* **18**, e0291506 (2023).

23. Wang, S. *et al.* Single-shot 20-fold expansion microscopy. *Nat. Methods* **21**, 2128–2134 (2024).

24. Valdes, P. A. *et al.* Improved immunostaining of nanostructures and cells in human brain specimens through expansion-mediated protein decrowding. *Sci. Transl. Med.* **16**, eabo0049 (2024).

25. Shin, T. W. *et al.* Dense, continuous membrane labeling and expansion microscopy visualization of ultrastructure in tissues. *Nat. Commun.* **16**, 1579 (2025).

26. Sim, J. *et al.* Nanoscale Resolution Imaging of Whole Mouse Embryos Using Expansion Microscopy. *ACS Nano* **19**, 7910–7927 (2025).

27. Wang, F. *et al.* iPEX enables micrometre-resolution deep spatial proteomics via tissue expansion. *Nature* 1–10 (2025) doi:10.1038/s41586-025-09734-0.

28. Glaser, A. *et al.* Expansion-assisted selective plane illumination microscopy for nanoscale imaging of centimeter-scale tissues. *eLife* **12**, (2024).

29. Steib, E. *et al.* TissUExM enables quantitative ultrastructural analysis in whole vertebrate embryos by expansion microscopy. *Cell Rep. Methods* **2**, (2022).

30. Bucur, O. *et al.* Nanoscale imaging of clinical specimens using conventional and rapid-expansion pathology. *Nat. Protoc.* **15**, 1649–1672 (2020).

31. Kylies, D. *et al.* Expansion-enhanced super-resolution radial fluctuations enable nanoscale molecular profiling of pathology specimens. *Nat. Nanotechnol.* **18**, 336–342 (2023).

32. Gao, R. *et al.* Cortical column and whole-brain imaging with molecular contrast and nanoscale resolution. *Science* **363**, eaau8302 (2019).

33. Hawkins, T. J., Robson, J. L., Cole, B. & Bush, S. J. Expansion Microscopy of Plant Cells (PlantExM). in *The Plant Cytoskeleton: Methods and Protocols* (eds Hussey, P. J. & Wang, P.) 127–142 (Springer US, New York, NY, 2023). doi:10.1007/978-1-0716-2867-6_10.

34. Grison, M. S. *et al.* Root expansion microscopy: A robust method for super resolution imaging in Arabidopsis. *Plant Cell* **37**, koaf050 (2025).

35. Lim, Y. *et al.* Mechanically resolved imaging of bacteria using expansion microscopy. *PLOS Biol.* **17**, e3000268 (2019).

36. Götz, R. *et al.* Expansion Microscopy for Cell Biology Analysis in Fungi. *Front. Microbiol.* **11**, (2020).

37. Bertiaux, E. *et al.* Expansion microscopy provides new insights into the cytoskeleton of malaria parasites including the conservation of a conoid. *PLOS Biol.* **19**, e3001020 (2021).